S³EPB

SLAC Summer School on Electron and Photon Beams

Measuring high brightness beams

C.Limborg-Deprey

U.S. DEPARTMENT OF ENERGY
Office of Science

SLAC NATIONAL ACCELERATOR LABORATORY

Introduction

Measuring e-beam properties

emittance, charge, monochromaticity, pulse duration …

$$B = \frac{Q}{\varepsilon_{n,x}\,\varepsilon_{n,y}\,\varepsilon_{n,z}}$$

$$B = \frac{Q}{\varepsilon_{n,x}^{2}\,\sigma_{\tau}\sigma_{E}}$$

Standard measurement techniques for tuning FELs

Some measurements of ultimate beam dimensions for colliders and e-diffraction sources

Synopsis

- Emittance definition
- Transverse emittance measurements
- Beam size measurements
  - Destructive
  - Non-Destructive
- Bunch lengths
  - Non-Destructive
  - Destructive
- Longitudinal Phase space

6D-emittance

Evolution of a population of particles (~10^9 for 160 pC) in time

3D-space coordinates (x, y, z) and their canonical (Hamilton) conjuguates (p_x,$\mathrm{p_y}$, p_z)

6D phase space of non-interacting particles,
in a conservative dynamical system
is invariant
→ "Liouville theorem"

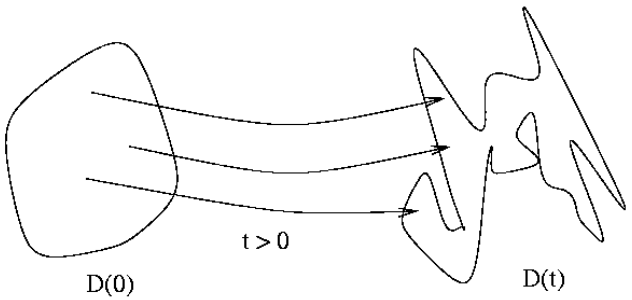

Volume $V = \int \psi(x, p_x, y, p_y, y, z, p_z)\, dx\, dp_x\, dy\, dp_y\, dz\, dp_z$ conserved

V referred to as emittance

J.D.Lawson "The physics of charge particle beams " , Clarendon Press, Oxford, 1977

6D-emittance – more practical choice of coordinates

Particles travel along z with relativistic velocity $v = \beta c$ and $p_z = \beta\gamma m_o c$

then $p_x = v_x \gamma m_o = \frac{dx}{dz}\frac{dz}{dt}\gamma m_o = x' \beta c\, \gamma m_o$

$$p_x \rightarrow \frac{p_x}{p_{zo}} = x'$$

$$p_y \rightarrow \frac{p_y}{p_{zo}} = y'$$

$$z \rightarrow \frac{(z - z_o)}{\beta c} = \tau$$

$$p_z \rightarrow \delta = \frac{p_z - p_{zo}}{p_{zo}} \text{ or } \delta = \frac{E - E_o}{E_o}$$

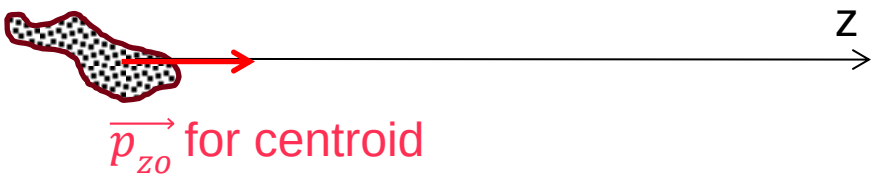

(x,x') are the trace-space coordinates (not conjuguate quantities)

$(x, p_x, y, p_y, y, z, p_z)$ → $(x, x', y, y', \tau, \delta)$ (measured quantities)

subtleties of emittance conservation are discussed in K.Floettmann , "some basic features of the beam emittance" PRST-AB Vol.3, 034202 (2003)

Geometric emittance / Normalized emittance

$$\varepsilon = \int f(x, x', y, y', \tau, \delta)\, dx\, dx'\, dy\, dy'\, d\tau\, d\delta$$

ε geometric emittance

ε conserved in the absence of acceleration

(ε decreases with $1/\gamma^3$ when beam accelerated)

we introduce $\varepsilon_n = \gamma^3 \varepsilon$, normalized emittance ε_n

ε_n conserved in the presence of acceleration

---------- Possible sources of emittance growth ----------

Non-linear space charge forces

Non-linear forces from electromagnetic components

Synchrotron radiation emission

Emittance - Practical evaluation

2D emittance : area occupied by particles represented in 2D “trace space”

What is the “area” for points ?

→ arbitrarily define a contour

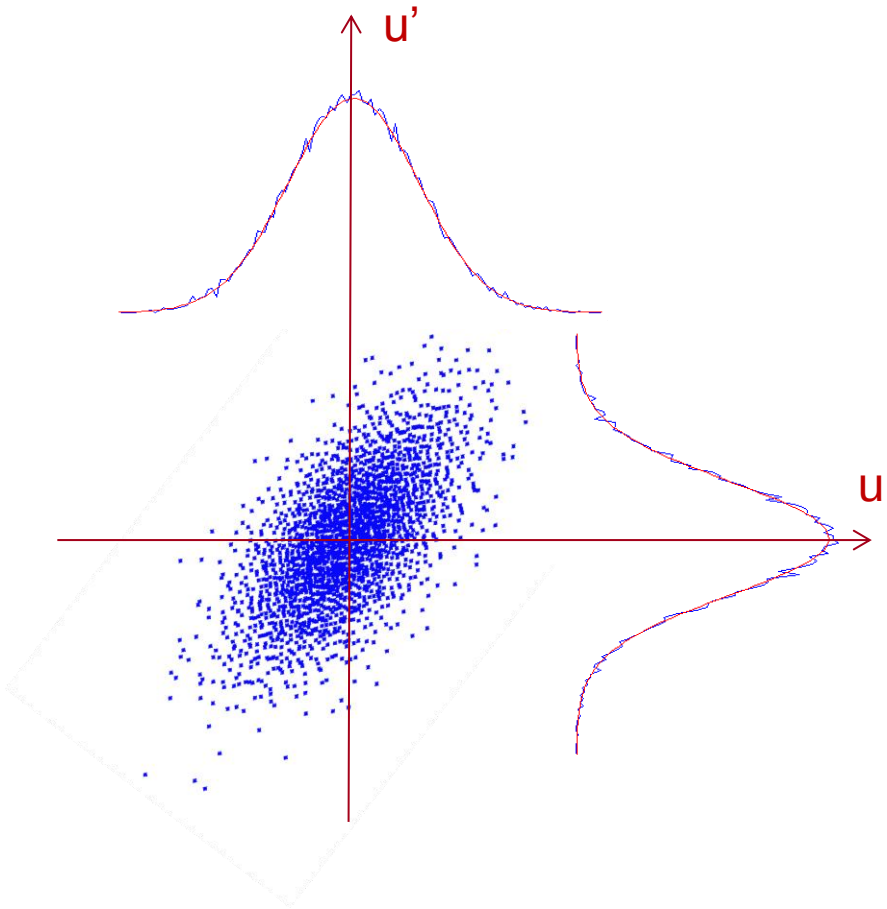

Typical distributions are gaussians,
or if not,
can be evaluated by their rms value ,

$$< u^2 > ,< u'^2 >,< uu' >$$

Emittance - Practical evaluation

- Determinant of the matrix of second order moments

$$\begin{vmatrix} < u^2 > & < uu' > \\ < uu' > & < u'^2 > \end{vmatrix}^{1/2}$$

$$\boxed{\varepsilon = \sqrt{< u^2 >< u'^2 > - < uu' >}}$$

used in our community

Corresponds to $\varepsilon = \frac{A}{\pi} = \sigma_M \, \sigma_m$

- Another definition : “Lapostolle”

$$\bar{\varepsilon} = 4\sqrt{< u^2 >< u'^2 > - < uu' >}$$

Corresponds to $\frac{A^*}{\pi} = 2\sigma_M \, 2\sigma_m$

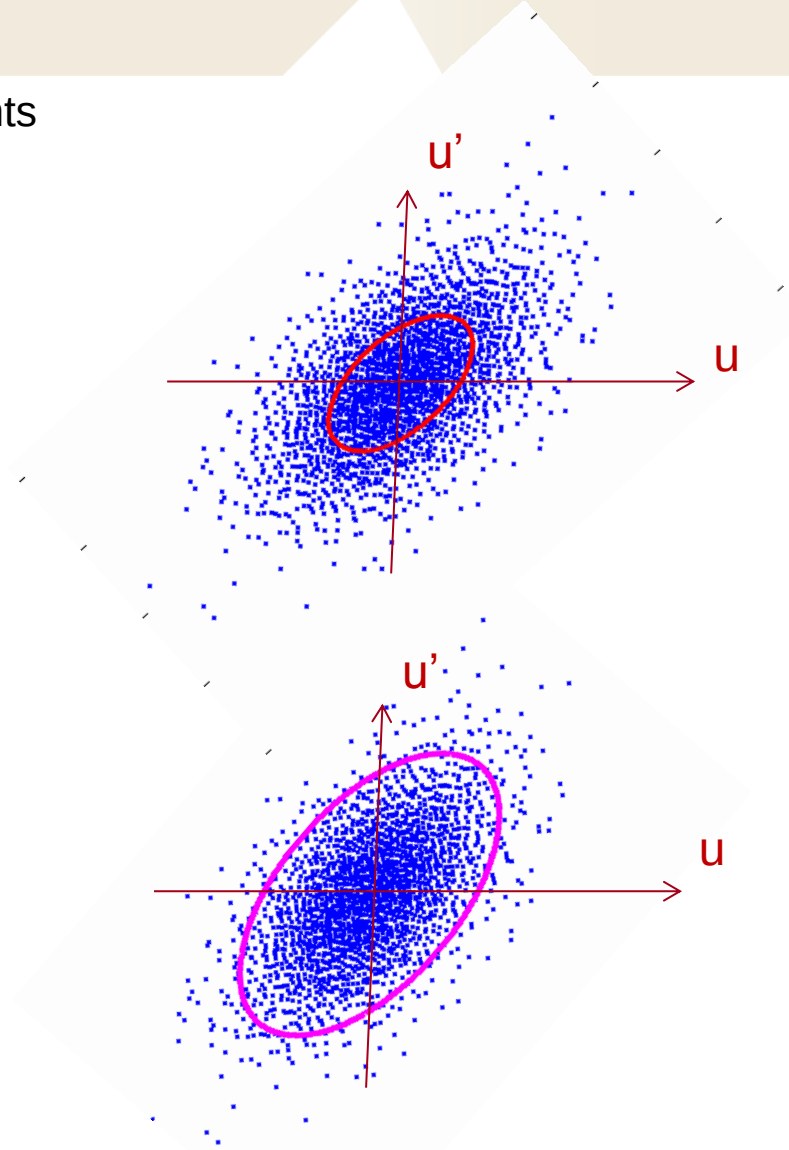

Emittance

Define Twiss parameters β, α, γ by

$$< u^2 > = \beta\varepsilon$$
$$< u'^2 > = \gamma\varepsilon$$
$$< uu' > = -\alpha\varepsilon$$

β, α, γ define the orientation of the ellipse

$\pi\varepsilon$ defines the area

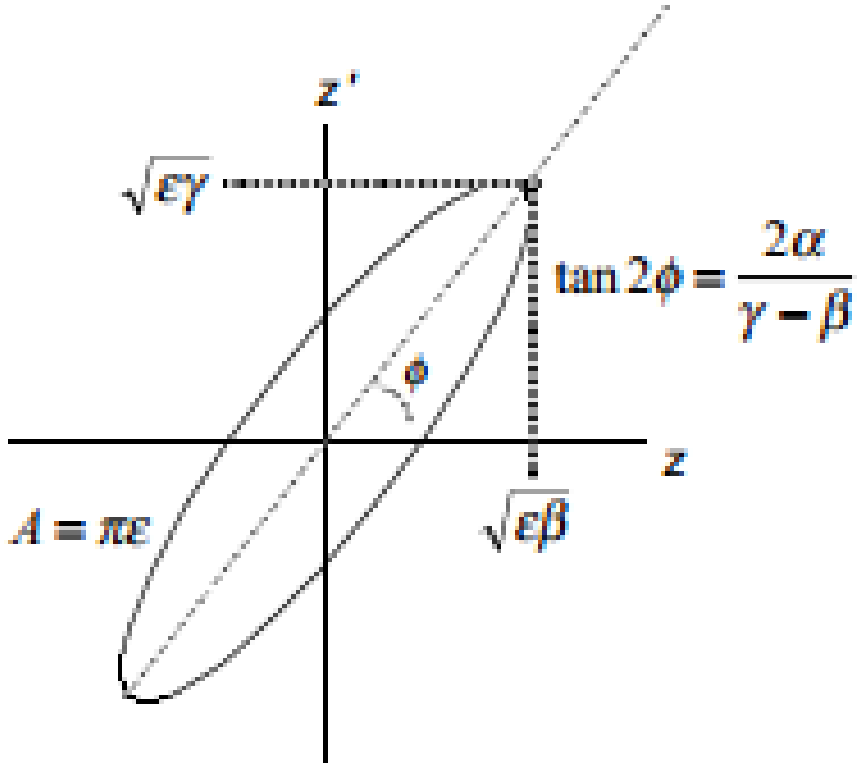

Courant-Snyder

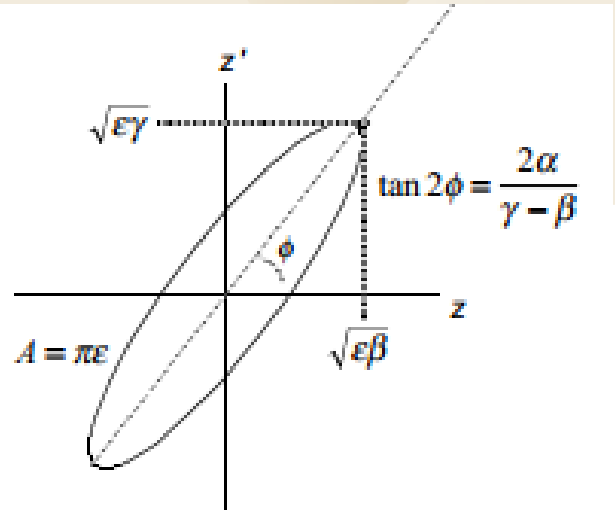

Another approach to emittance

Particles (u,u') subject to restoring forces K(s) u

$u'' + K(s)u = 0$ Hill's equation

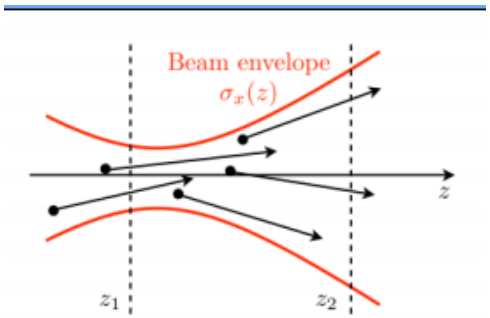

Solution: $u(s) = \sqrt{\varepsilon\beta(s)}\, sin(\psi(s) + \phi_o)$

with $\psi(s) = \int_{s_o}^{s} \frac{ds'}{\beta(s')}$

ε and ϕ_o are constants of integration

Defining : $\alpha(s) = -\frac{1}{2}\beta'(s)$ and $\gamma(s) = \frac{1+\alpha^2(s)}{\beta^2(s)}$

$\gamma(s)u^2(s) + 2\alpha(s)u(s)u'(s) + \beta(s)u'^2(s)$ = constant (Courant-Snyder Invariant) = ε

Also equation of an ellipse

Explains why choice of an ellipse is more than a mathematical convenience

Measuring emittance

$$\varepsilon = \sqrt{< u^2 >< u'^2 > - < uu' >}$$

Beam size

Beam divergence

Correlation
Position-angle

One method gives the 3 parameters in one shot : “Pepper pot”
but

destructive
only for low energy beam (E < 10 MeV)

Pepper pot

Transverse emittance , low energy
Destructive
Single Shot

Multislit in high Z material

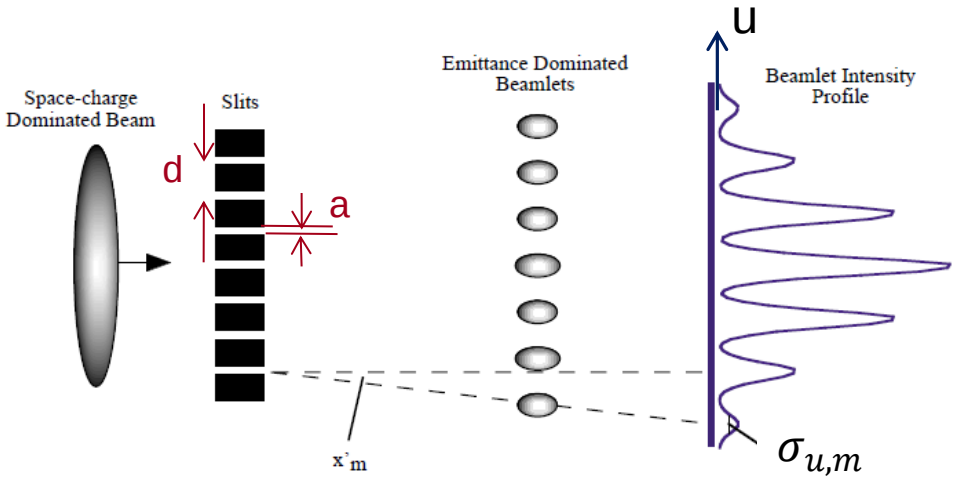

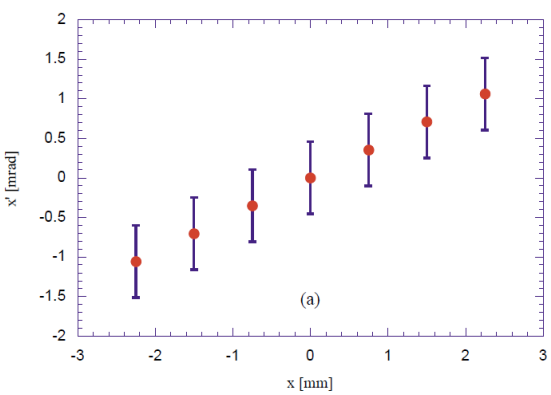

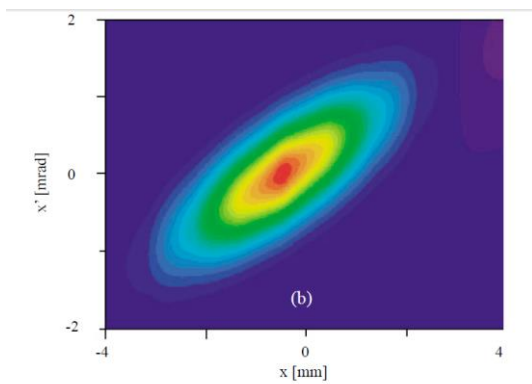

FIG. 2. (Color) (a) Beam trace space constructed from the beamlet intensity profile illustrated in Fig. 1. Each point represents the position of a beamlet in trace space and the error bars indicate the thermal spread of the beamlets. (b) Contour plot representation of the same data. Here the relative weights of the beamlets are resolved.

Direct reading of trace space

$$u'_m = x'_m = \frac{u_m - x_m}{L} = \frac{u_m - md}{L}$$

$$\sigma'^2_m = \sigma^2_{u,m} - \left(\frac{a}{4}\right)^2$$

$$< x^2 > = \frac{\sum I_m x_m^2}{\sum I_m},$$

$$< x'^2 > = \frac{\sum I_m \left(x'^2_{m,o} + \frac{\sigma'^2_m}{L^2}\right)}{\sum I_m},$$

$$< xx' > = \frac{\sum I_m x_{m,o} x'_{m,o}}{\sum I_m}$$

With I_m detected intensity for m^{th} beamlet

M. Zhang, Report No. FERMILAB-TM-1988, 1996
S. G. Anderson, et al. Phys. Rev. ST Accel. Beams 5, 014201 (2002)

Pepper pot for thermal emittance

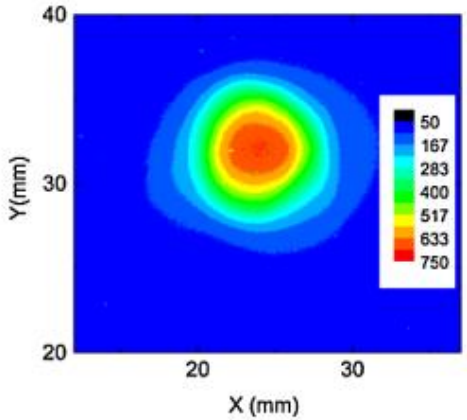

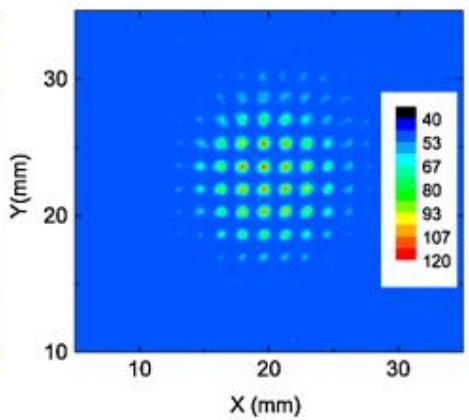

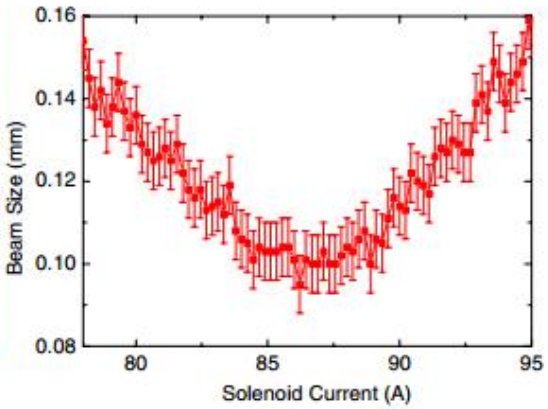

Electron beam on YAG, with pepper pot in, Solenoid scan

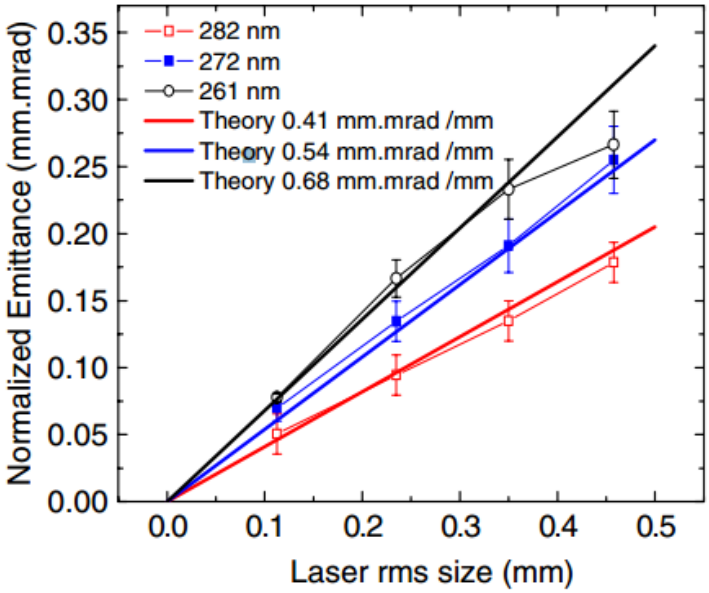

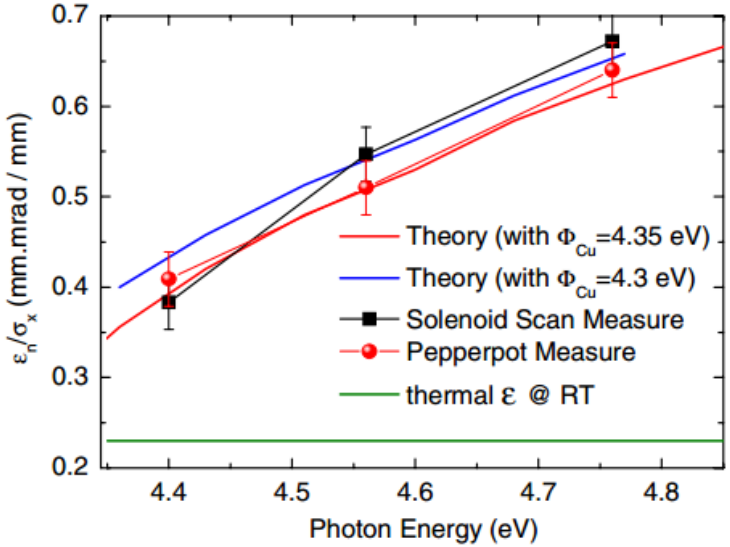

C.P.Hauri , PRL 104, 234802 (2010)

Pepper pot based emittance oscillation

Emittance-meter
Variation of emittance along z after gun (at 5 MeV)

2mm thick W
7 slits of ~ 50 μm at 500 μm
Resolution ~ 100 μrad

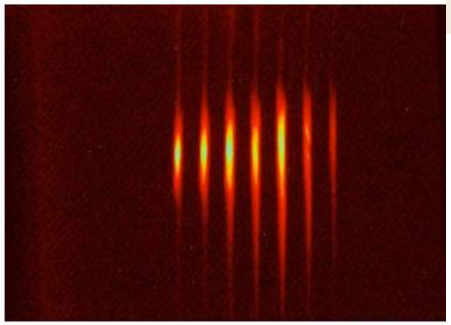

PITZ data

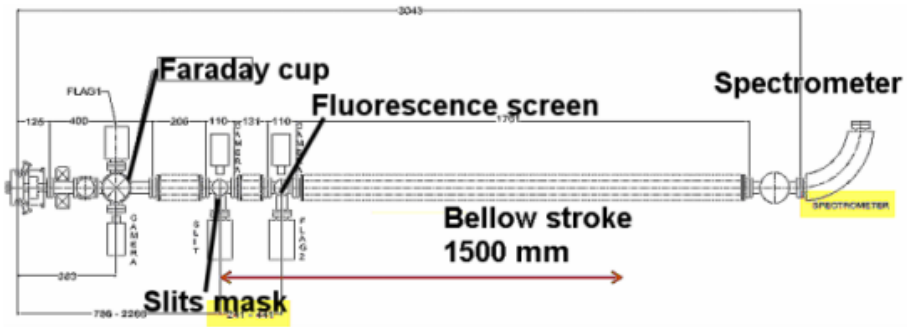

Figure 2: Emittance-meter design.

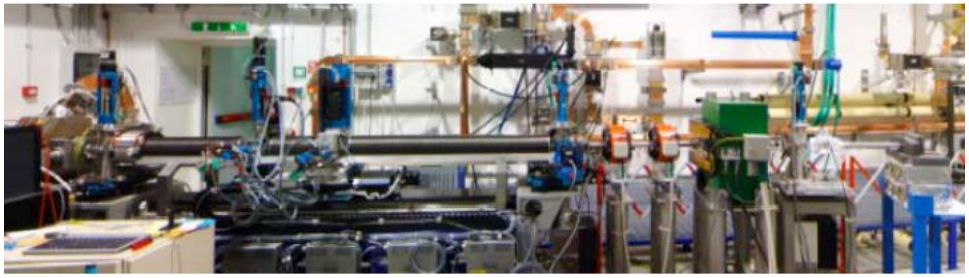

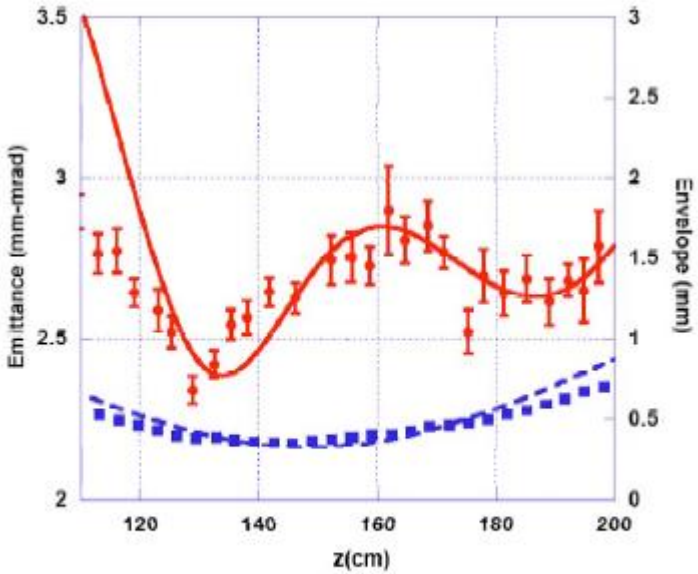

Figure 5: Envelope and Emittance downstream the RF gun of a "flat top" bunch.

D.Alesini et al , "Experimental results with the SPARC emittance-meter" MOOAAB02, PAC07

Photofield emission from tips : Nb/ Nb3Sn

No explosive electron emission erosion

even if close to 1GW/cm^2 limit

Huge QE ~ 0.9 % (X 100)

ε_n = 0.6 mm-mrad at 2500pC

Brightness better by ~ 100

than conventional PC guns

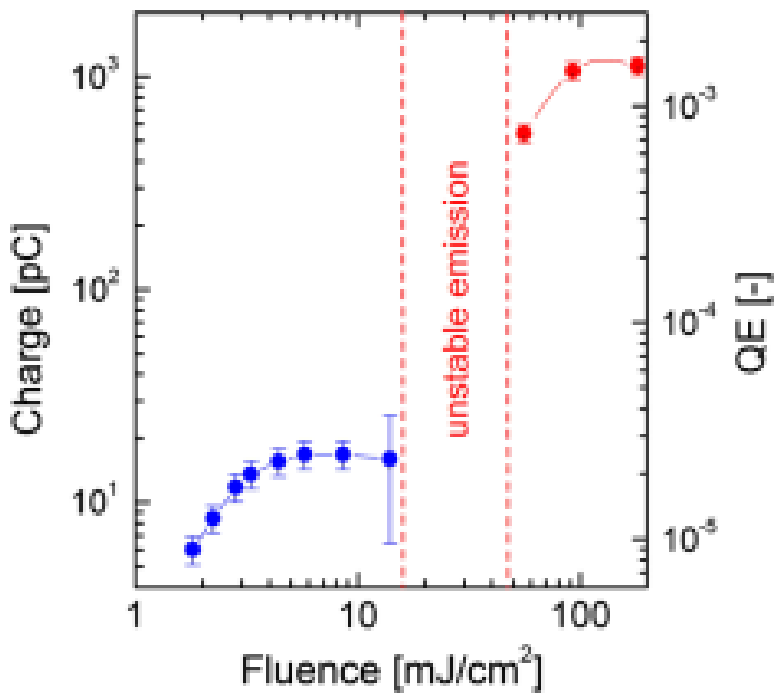

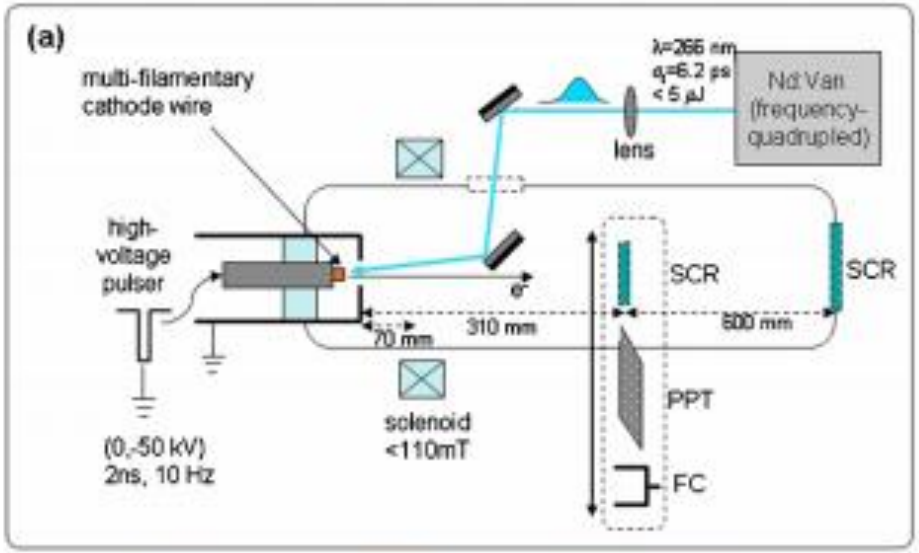

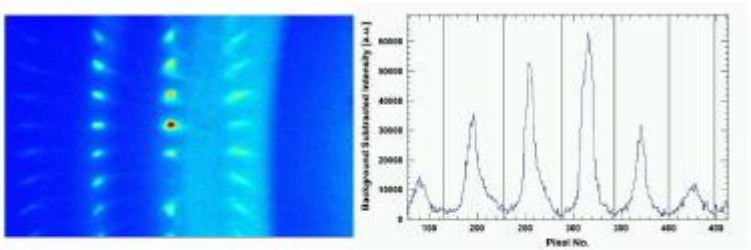

FIG. 8 (color online). (Left panel) Typical pepperpot beamlets recorded on a YAG screen. (Right panel) Cross section used for emittance calculation with XANAROOT [17].

A.Anghel et al , PRL , 108, 194801 (2012)

Pepper pot

Transverse emittance , low energy
Destructive
Single Shot

- **Difficult at high energy**
  scattering stopping length longer with energy :

$$L_s[cm] = \frac{E}{dE/dx} \cong \frac{E[MeV]}{1.5\,\rho[g.cm^{-3}]}$$

	W	Ta	Cu
[g/cm³]	15.6	16.7	8.96

E > 10 MeV , L_s ~ 5 mm

- **Unsuitable for extremely low emittance**
  slit thickness condition : $\sigma_{x'} < \frac{a}{4w}$
  minimum emittance ∝ a (slit width) but S/N decreases

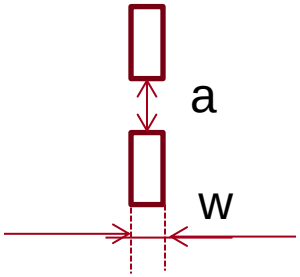

- **Space Charge correction**: low energy : analysis still often requires space charge calculation

G. Anderson, et al. Phys. Rev. ST Accel. Beams 5, 014201 (2002)

Grid for low emittance

Transverse emittance , low energy
Destructive
Single Shot

Measuring extremely low emittance <0.1 mm-mrad

Grid technique similar to pepper pot ,

multi knife edge measurement with info. on correlations

electrons hitting Cu bars scattered at wide angle

huge magnification M= 12.8 (from L =2 m)

$$M\,a > L\,\sigma'_m$$

a : bar width = 32 μm

L : distance grid to screen =2.1m

σ'_m : divergence of beamlet ~40 μrad

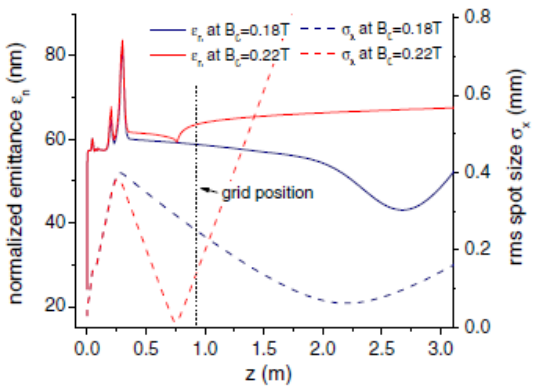

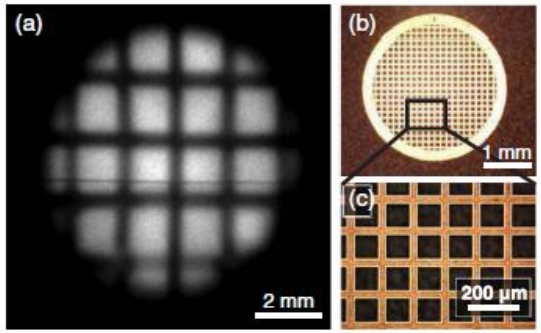

FIG. 5. (a) Electron beam shadow image on the detector screen 2.1 m after the TEM grid. The image of the grid appears magnified by a factor of 12.8. (b), (c) Optical microscope images of the 200 mesh TEM grid.

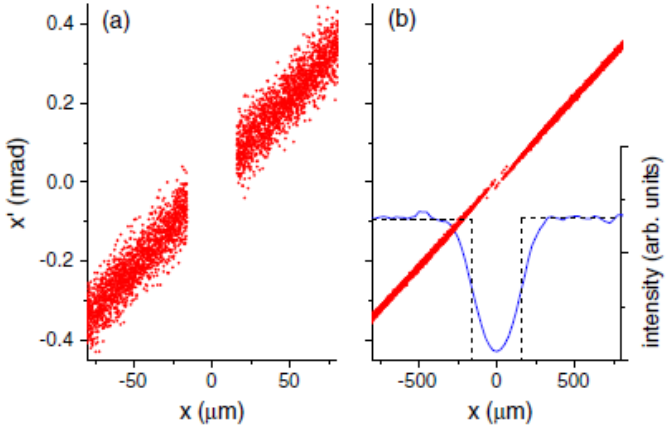

30nm measured with 0.1 pC

R.Li et PRST-AB 15, 090702 (2012)

Grid for low emittance

Transverse emittance , low energy
Destructive
Single Shot

Studying cigar shape :

linear space charge

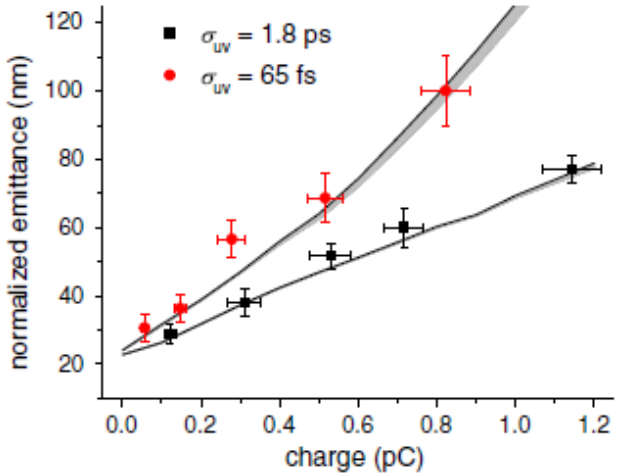

FIG. 7. Measured normalized emittance of beams when the UV laser was stretched to a 1.8 ps rms parabolic longitudinal profile (black square) and was ultrashort at 65 fs rms (red circle). The error bars indicate the statistics over 20 shots. Simulation results for both cases are also shown.

Profile measured GPT Simulations

1.8ps

65fs

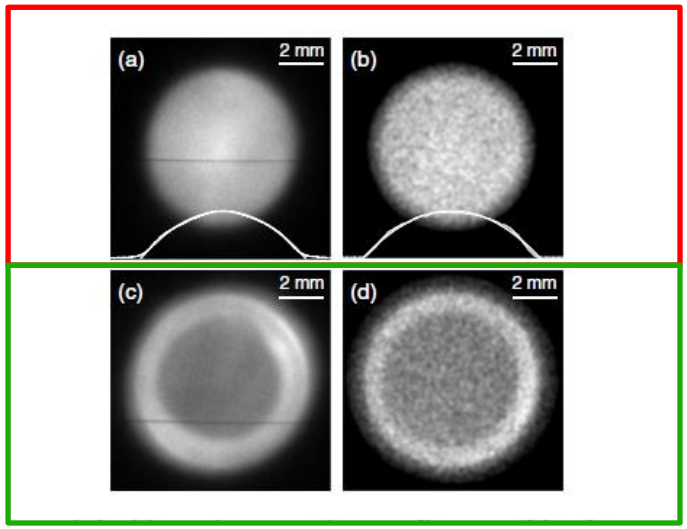

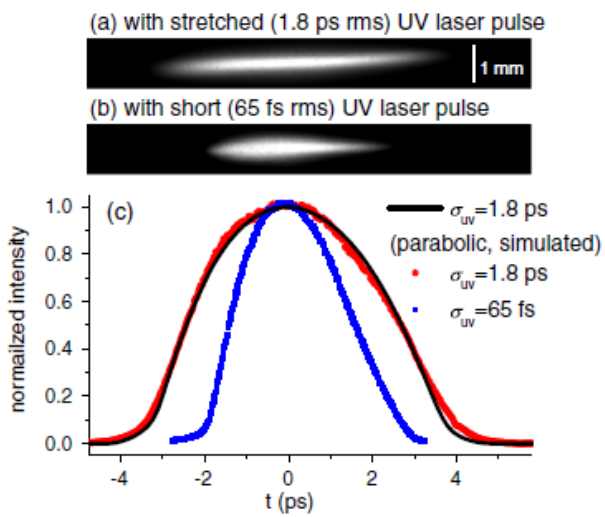

R.Li et PRST-AB 15, 090702 (2012)

"Quad" scan

Transverse emittance
Destructive
Multi Shot

Quadrupole/solenoid scan

$$\begin{pmatrix} x \\ x' \end{pmatrix} = \begin{pmatrix} 1 & L \\ 0 & 1 \end{pmatrix} \begin{pmatrix} 1 & 0 \\ -\frac{1}{f} & 1 \end{pmatrix} \begin{pmatrix} x_o \\ x'_o \end{pmatrix} = R \begin{pmatrix} x_o \\ x'_o \end{pmatrix}$$

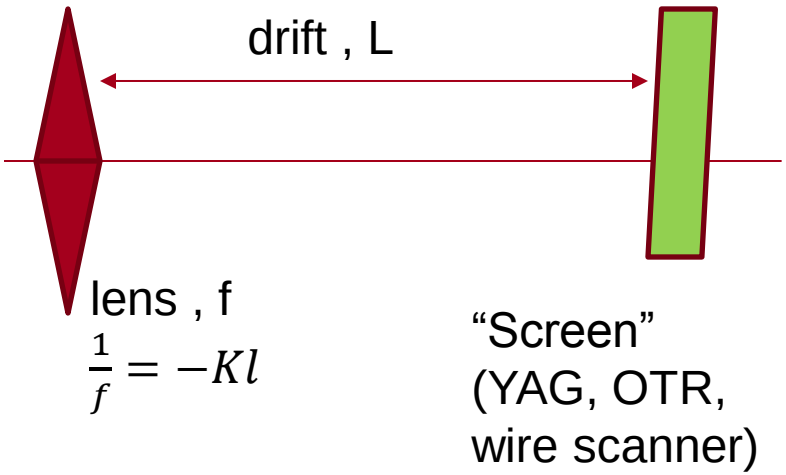

$$\begin{cases} x = \left(1 - \frac{L}{f}\right) x_o + L x_o \\ x' = -\frac{x_o}{f} + x'_o \end{cases}$$

$$\langle x^2 \rangle = \left(1 - \frac{2L}{f} + \frac{L^2}{f^2}\right) \langle x_o^2 \rangle + 2L \left(1 - \frac{L}{f}\right) \langle x_o x'_o \rangle + L^2 \langle x'^2_o \rangle$$

$$\langle x^2 \rangle = \frac{a}{f^2} + \frac{b}{f} + c$$

Solve for a,b,c to determine $\langle x_o^2 \rangle, \langle x_o x'_o \rangle, \langle x'^2_o \rangle$

$$\varepsilon = \sqrt{\langle x_o^2 \rangle \langle x'^2_o \rangle - \langle x_o x'_o \rangle}\,,\ \alpha = -\frac{\langle x_o x'_o \rangle}{\varepsilon}\,,\ \beta = \frac{\langle x_o^2 \rangle}{\varepsilon}\,,\ \gamma = \frac{\langle x'^2_o \rangle}{\varepsilon}$$

"Quad" scan

Transverse emittance
Destructive
Multi Shot

$$\begin{pmatrix} \sigma_{x_1}^2 \\ \sigma_{x_2}^2 \\ \cdots \\ \cdots \\ \sigma_{x_n}^2 \end{pmatrix} = \begin{pmatrix} R_{11,1}^2 & 2R_{11,1}R_{12,1} & R_{12,1}^2 \\ \cdots & \cdots & \cdots \\ \cdots & \cdots & \cdots \\ \cdots & \cdots & \cdots \\ R_{11,n}^2 & 2R_{11,n}R_{12,n} & R_{12,n}^2 \end{pmatrix} \begin{pmatrix} \beta_o\varepsilon \\ -\alpha_o\varepsilon \\ \gamma_o\varepsilon \end{pmatrix}$$ also written $\Sigma = BO$

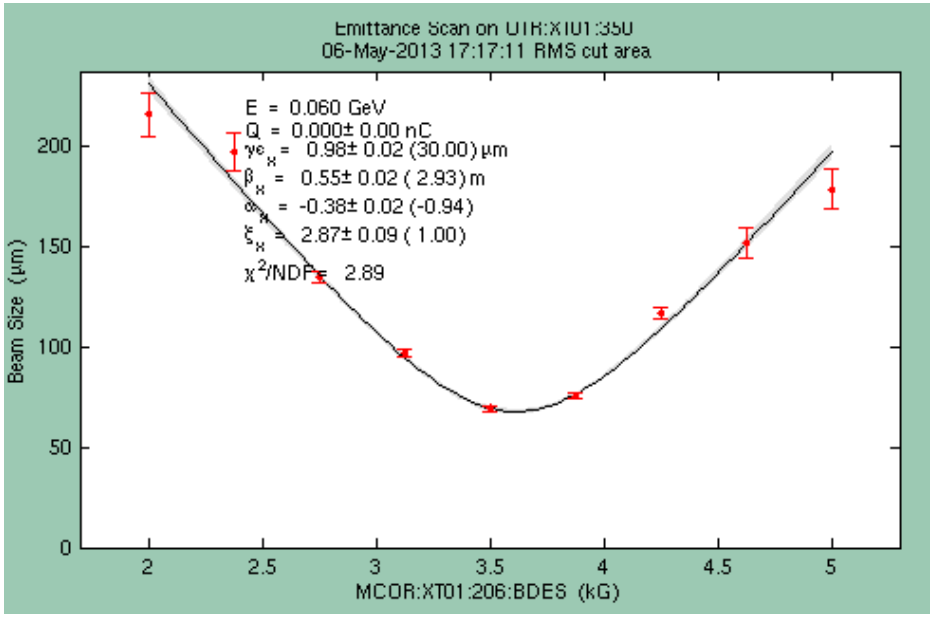

Solve for O by least square fit

Minimization of $\chi^2 = \sum_i \frac{1}{\sigma_{x_i}^2}\left(\sigma_{x_i}^2 - \sum_j B_{ij}\, O_j\right)^2$

Error analysis

Calculate covariant matrix $T = \left(\hat{B}^T\hat{B}\right)^{-1}$

where $\hat{B}_{ij} = \frac{B_{ij}}{\sigma_{x_i}^2}$

Solution is $O = T\hat{B}^T\hat{\Sigma}$ where $\hat{B}_{ij} = \frac{B_{ij}}{\sigma_{x_i}^2}$ and $\hat{\Sigma}_i = \sigma_{x_i}^2$

Error $\sigma_{O,i} = \sqrt{T_{ii}}$

Reference "F.Zimmermann, M.Minty, " book ref.
H.Loos , private communications

"Quad" scan

Transverse emittance
Destructive
Multi Shot

- Choice of quadrupole settings

At each data point , plot lines parametrized in x'_i

$$\begin{pmatrix} u \\ u' \end{pmatrix} = R \begin{pmatrix} \sigma_{x_i} \\ x'_i \end{pmatrix}$$

Optimum location of data points

over-constrain (N points > 3)

at least 3 separated by more than 45 degrees

typically ~ 7 points , covering more than 90 degrees

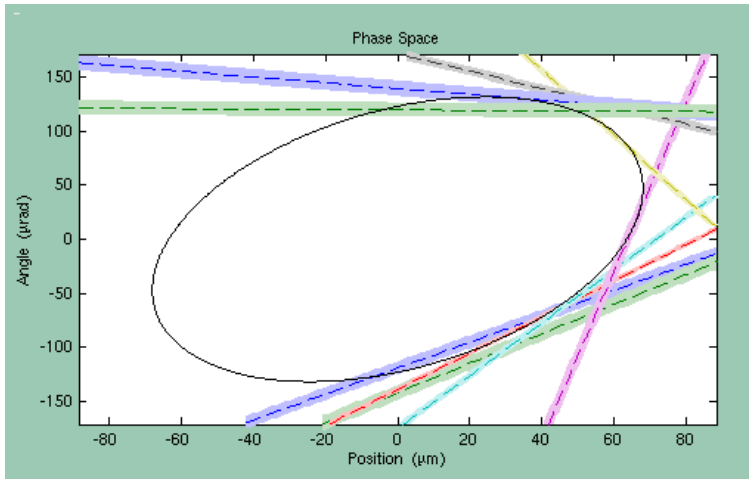

- Convenient representation in normalized/rotated phase space

$\left(\frac{x}{\sqrt{\beta}}, \frac{\alpha x + \beta x'}{\sqrt{\beta}}\right)$ where (α, β) Twiss design parameters

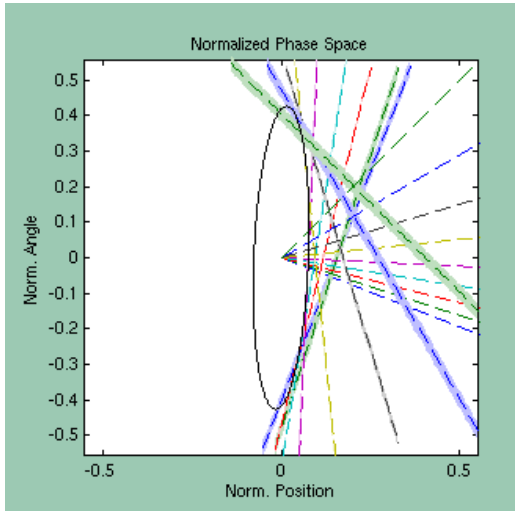

“Quad” scan

Transverse emittance
Destructive
Multi Shot

- Low energy or high density

strong space charge,

R to include space charge defocusing term (beam size dependent)

$$R_{sc}(\Delta s) = \begin{pmatrix} 1 & 0 & 0 & 0 & 0 & 0 \\ \Delta s/f_{sc,x} & 1 & 0 & 0 & 0 & 0 \\ 0 & 0 & 1 & 0 & 0 & 0 \\ 0 & 0 & \Delta s/f_{sc,y} & 1 & 0 & 0 \\ 0 & 0 & 0 & 0 & 1 & 0 \\ 0 & 0 & 0 & 0 & \Delta s/f_{sc,z} & 1 \end{pmatrix}$$

$$1/f_{sc,x} = K/2\left[\frac{1}{5}\frac{1}{X^2}\right]^{3/2} R_d\left[\frac{Y^2}{X^2}, \frac{Z^2}{X^2}, 1\right]$$

$$1/f_{sc,y} = K/2\left[\frac{1}{5}\frac{1}{Y^2}\right]^{3/2} R_d\left[\frac{Z^2}{Y^2}, \frac{X^2}{Y^2}, 1\right]$$

$$1/f_{sc,z} = K/2\left[\frac{1}{5}\frac{1}{Z^2}\right]^{3/2} R_d\left[\frac{X^2}{Z^2}, \frac{Y^2}{Z^2}, 1\right]$$

$$K = \frac{qN}{2\pi\varepsilon_0}\frac{1}{\gamma^3\beta^2}\frac{q}{mc^2}$$

Use iterative methods

C.K. Allen “Theory and Technique of Beam Envelope Simulation”, LANL, LA-UR-02-4979 August 2002
C.Limborg, “A Modified Quad Scan technique for space charge dominated beams”, PAC03 , http://accelconf.web.cern.ch/AccelConf/p03/PAPERS/WPPG033.PDF

Slice emittance

Slice emittance
Destructive
Multi Shot

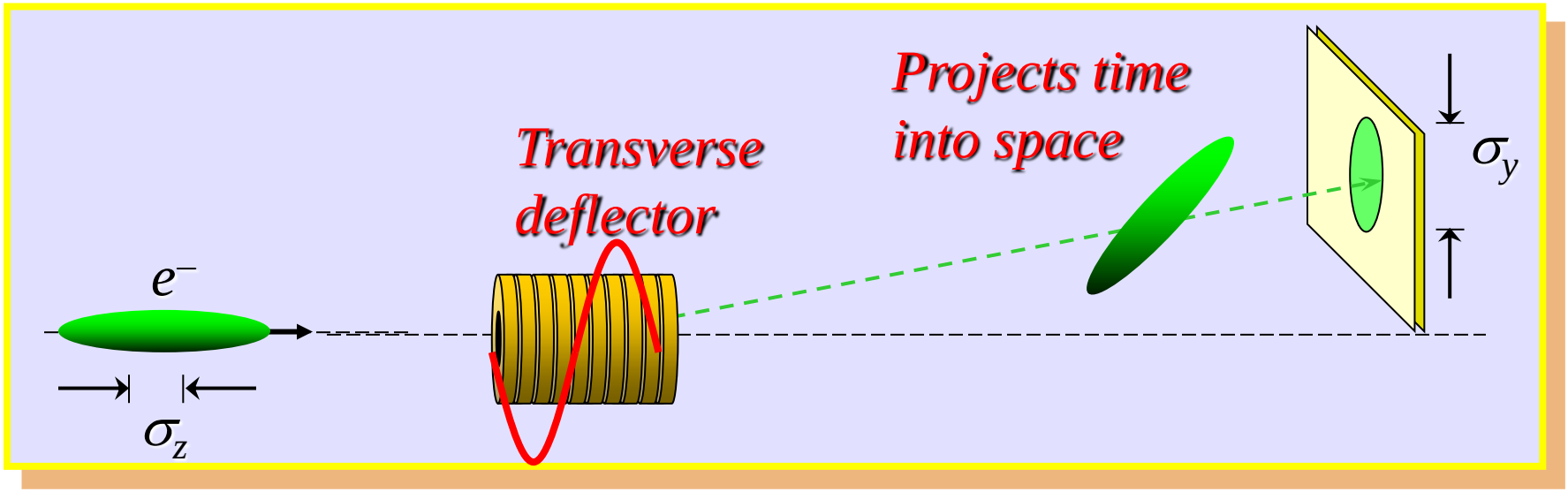

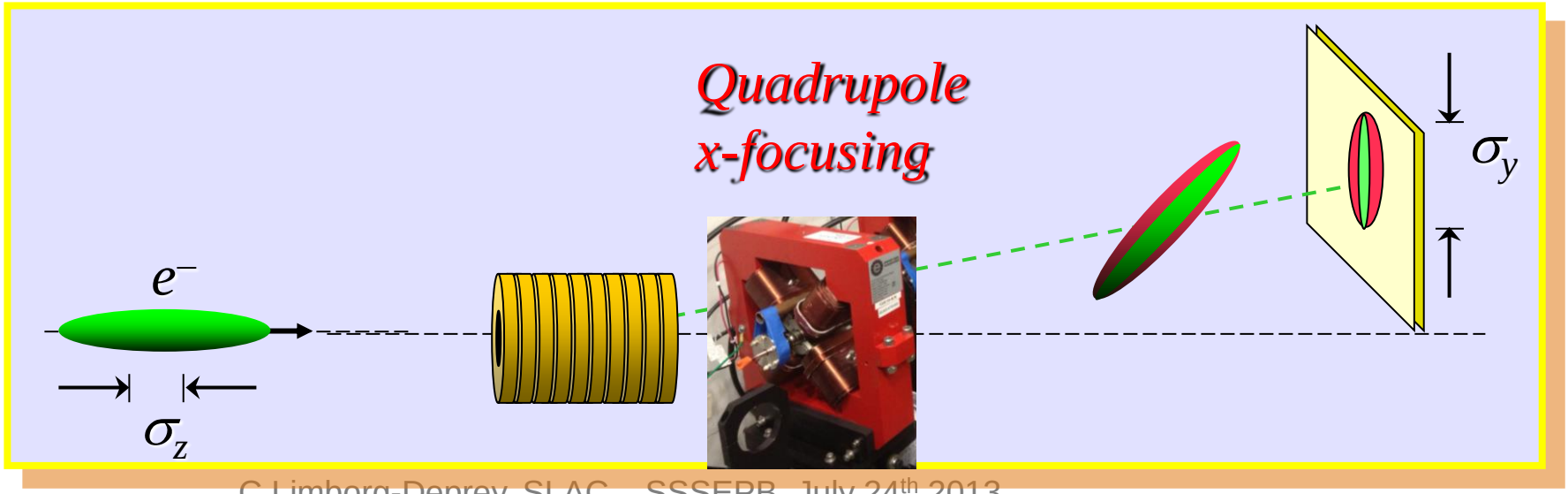

Slice emittance

Slice emittance
Destructive
Multi Shot

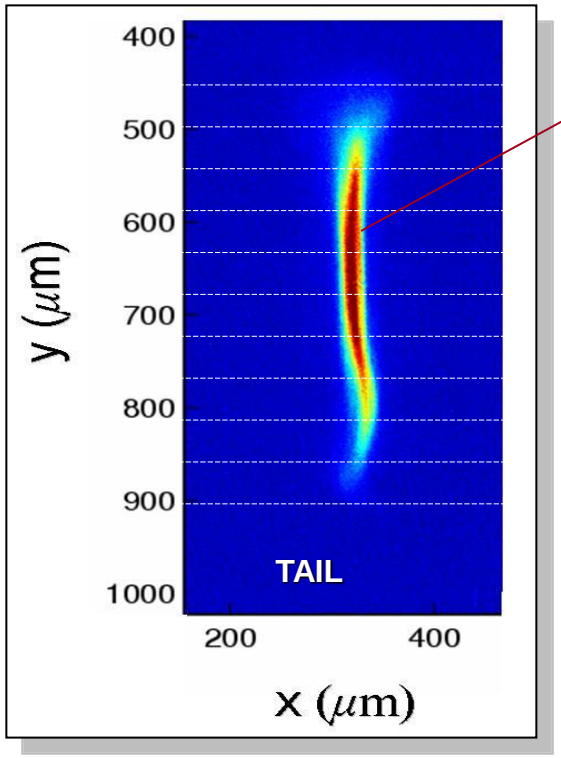

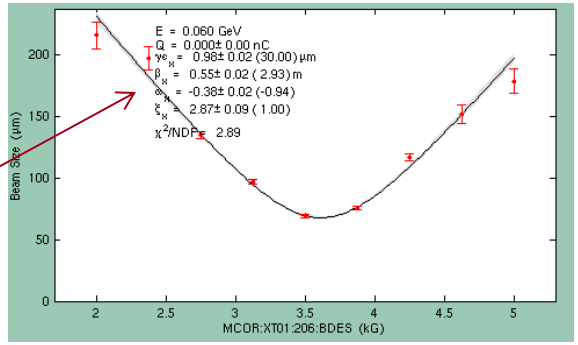

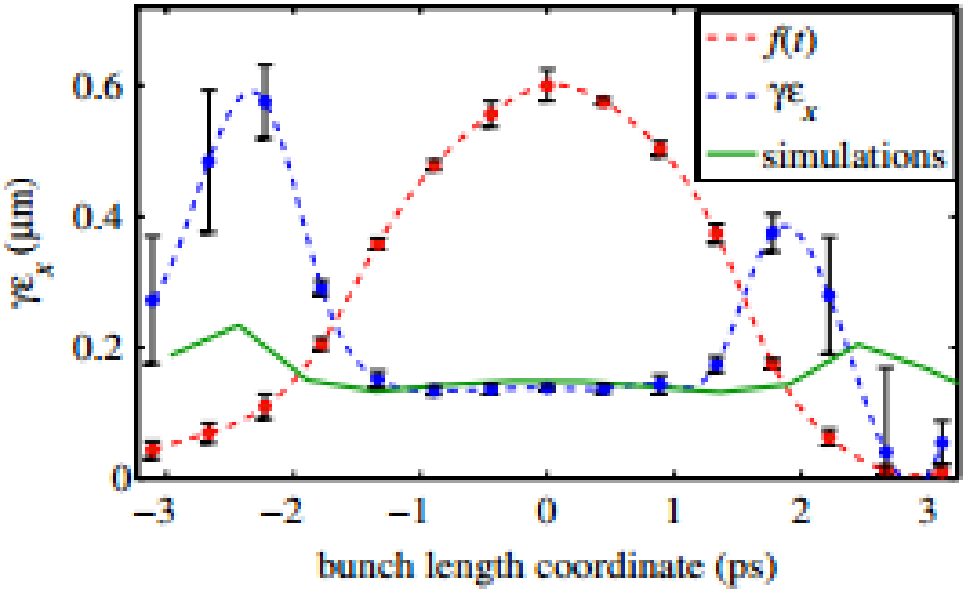

Thermal emittance

Transverse emittance
Destructive
Multi Shot

- Thermal emittance measurement from slice emittance as a function of laser spot size (at low charge ~20pC)
- LCLS gun : copper (robustness, long lifetime)
- 0.9 mm-mrad per mm rms from slice emittance measurement

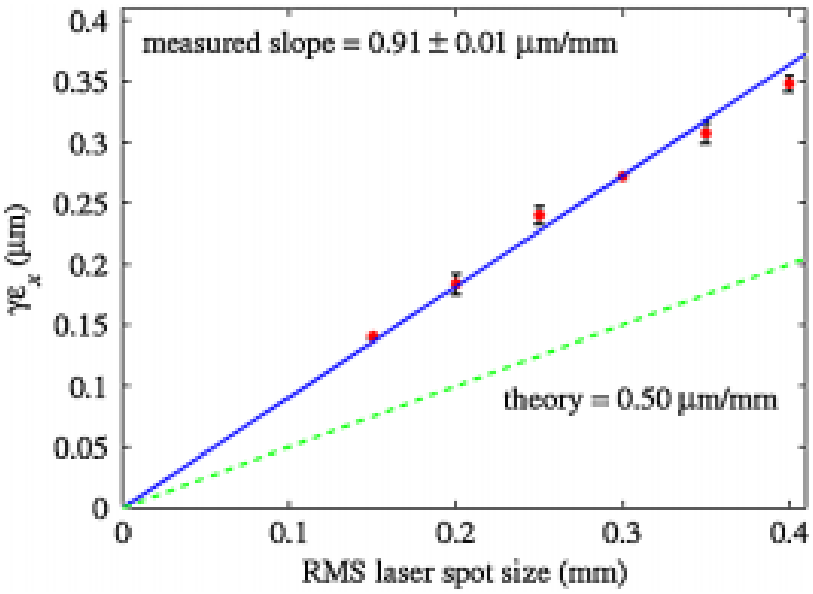

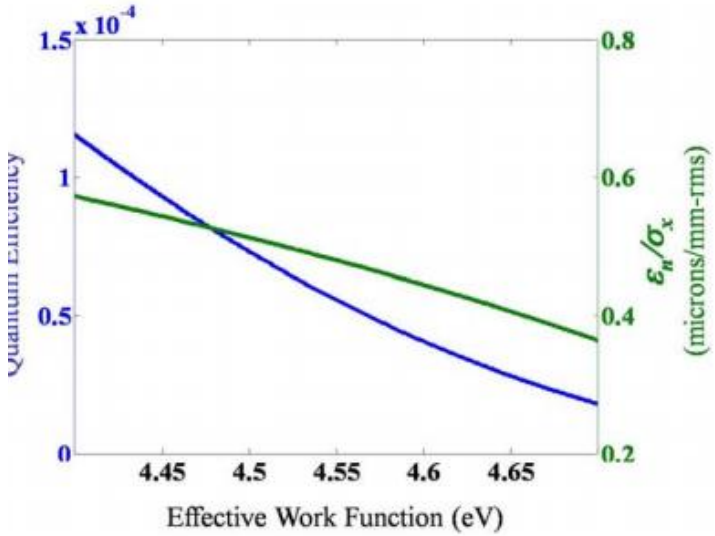

m efficiency and the normalized emittance per rms beam size plotted a
, ϕ_{eff}, for a photon energy of 4.90 eV (λ_{laser} = 253 nm).

Thermal emittance

Transverse emittance
Destructive
Multi Shot

- Thermal emittance measurement from photoinjector

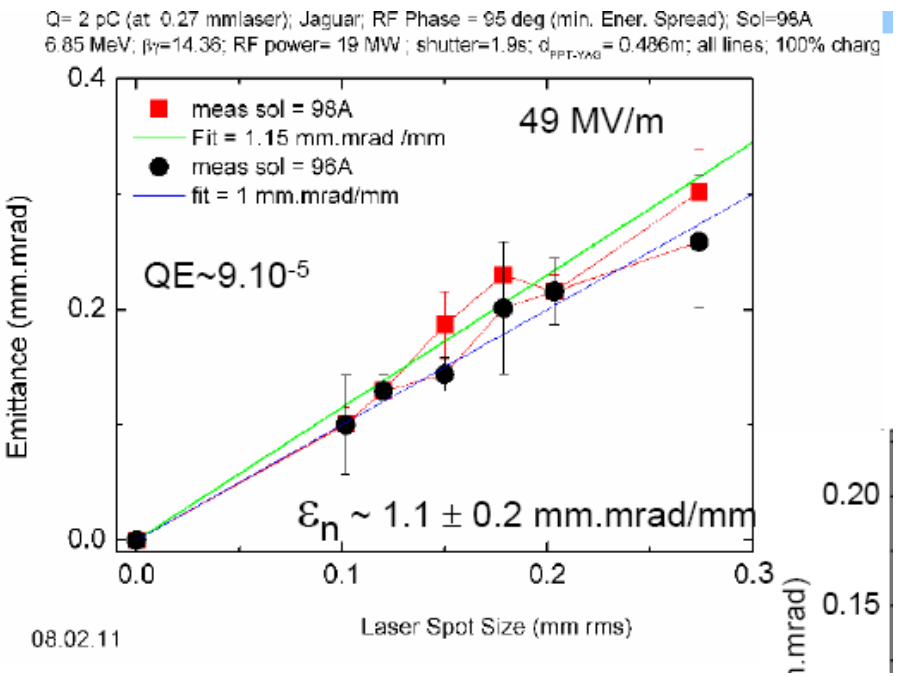

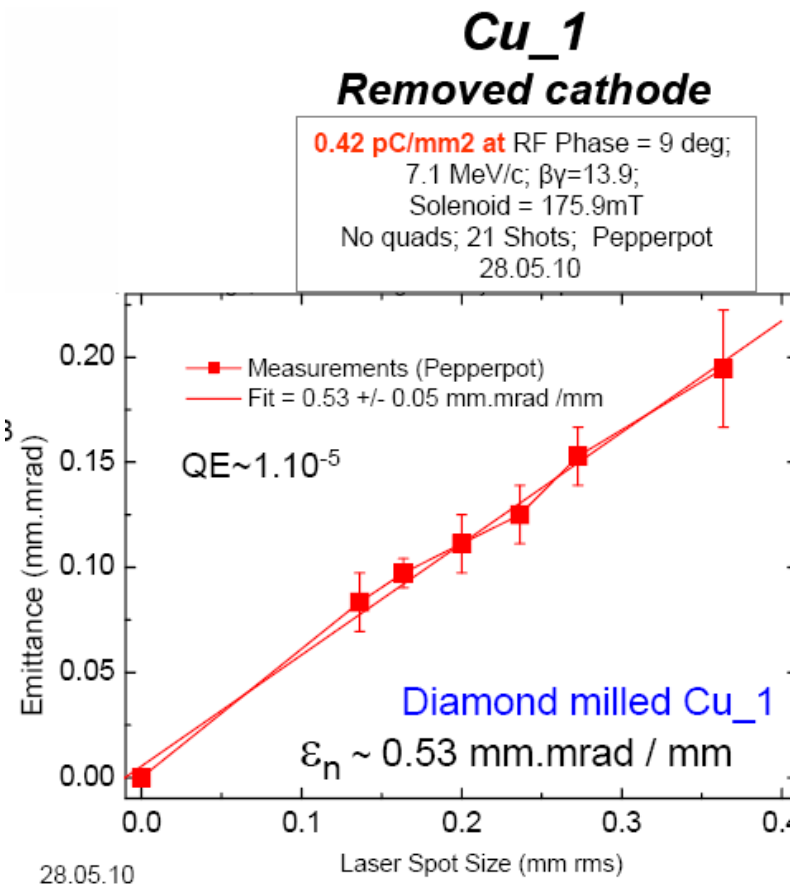

Courtesy F.LePimpec, R.Ganter

Thermal emittance

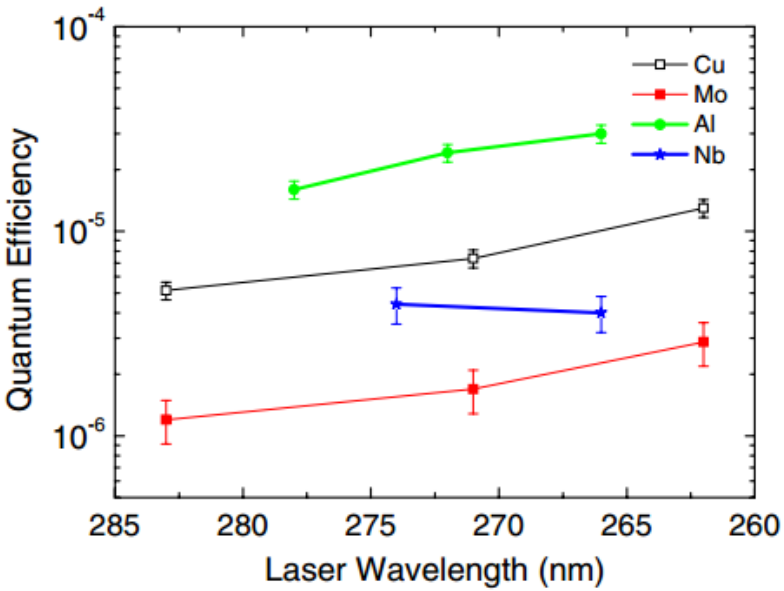

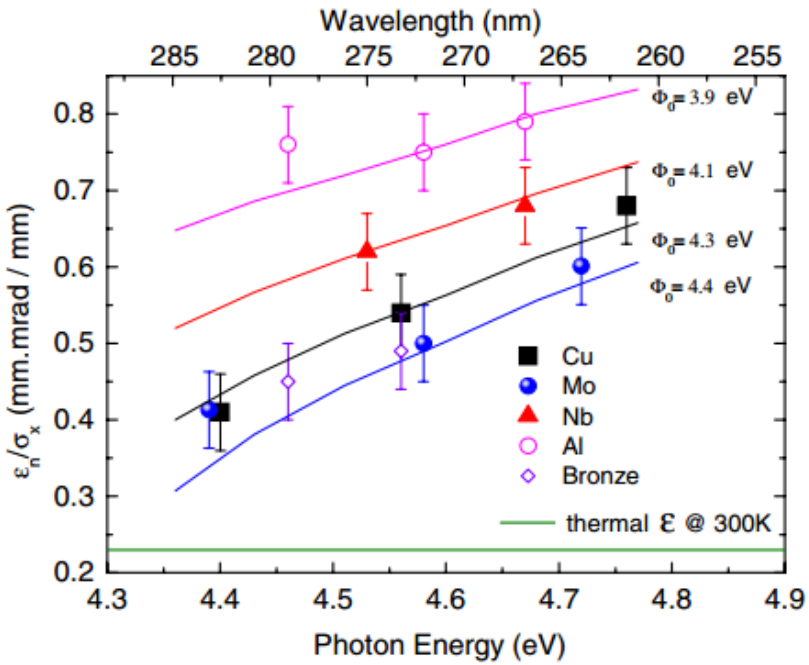

$$QE \sim (h\nu - \Phi_{eff})^2$$

$$\varepsilon_{nx} \sim \sqrt{h\nu - \Phi_{eff}}$$

C.P.Hauri , PRL 104, 234802 (2010)

Emittance , Temperature , Coherence Length

$\varepsilon_n = \sigma_x \frac{\sigma_{px}}{mc}$ for e-source

$\varepsilon_n = \sigma_x \sqrt{\frac{k_b T}{mc^2}}$ transverse velocities expressed in terms of temperature

Typical numbers for photo-injectors (metallic or semi-conductor):

$$\varepsilon_n = 0.9\, mm - mrad\ per\ mm\ rms$$

T = 4809 K , $k_b T = 0.41\ eV$

FELs, linear colliders : small beam size collimated beam

"geometric emittance" $\varepsilon = \frac{\varepsilon_n}{\gamma}$ small at high γ and small ε_n

For electron diffraction community, coherence length

$L_c = \frac{\lambda}{2\pi\sigma_\theta} = \frac{\hbar}{mc} \frac{\sigma_x}{\varepsilon_{n,x}}$ L_c needs to be many lattice spacing

example: $\varepsilon_n = 0.02\, mm - mrad$

$\sigma_x = 0.2\, mm$

Lc = 4 nm

Quality of source measured in $C_\perp = \frac{L_\perp}{\sigma_x}$

Cold Electron source

N ~ 10^8 Rb atoms
R = 1mm
T = 230 μK

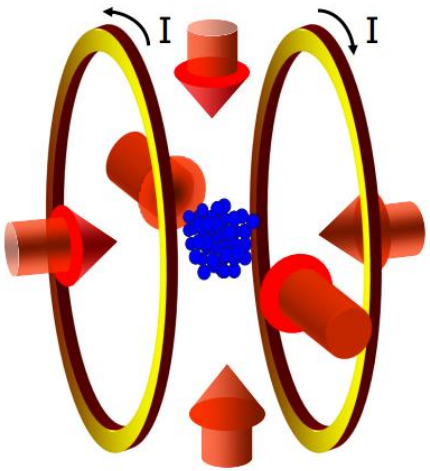

Magneto-Optical Trap (MOT)

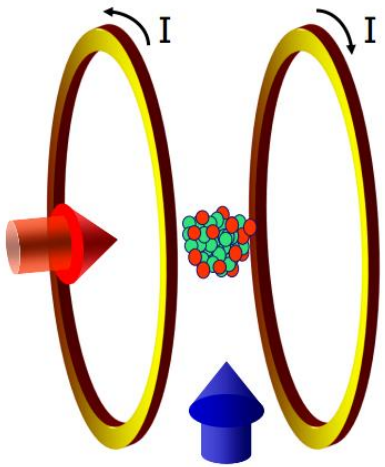

Ultracold Plasma

Killian et al., PRL **83**, 4776 (1999)

Electron temperature

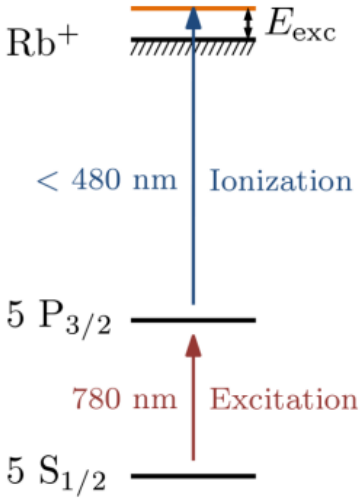

$$kT_e \approx \frac{\hbar}{\tau}$$

plasma effects

$$\rightarrow T_e \approx 10\ \mathrm{K}$$

Courtesy O.J.Luiten

Cold Electron source

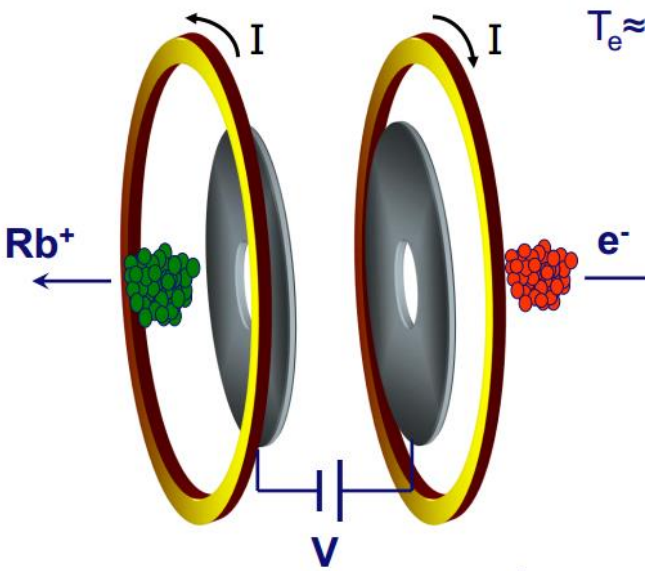

Ultracold beams!

Courtesy O.J.Luiten

Electron temperature

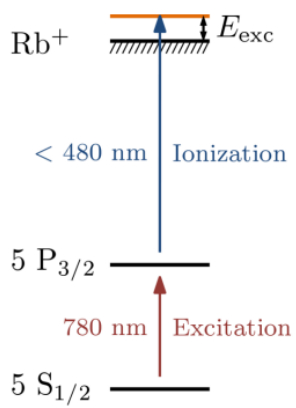

$$kT_e \approx \frac{\hbar}{\tau}$$

plasma effects

$\rightarrow T_e \approx 10$ K

Conventional photo and field emission fields

$T_e \approx$ 5000 K (0.5 eV) $\rightarrow$ 20K

$$\varepsilon_n = \sigma_x \sqrt{\frac{k_b T}{mc^2}}$$

$$T \equiv \frac{\sigma_p^2}{mk_b}$$

T = 5000 K for 0.9 mm-mrad per rms mm

T = 1500 K for 0.5 mm-mmrad per rms mm

Solenoid scan
for extremely small emittance

Solenoid scan

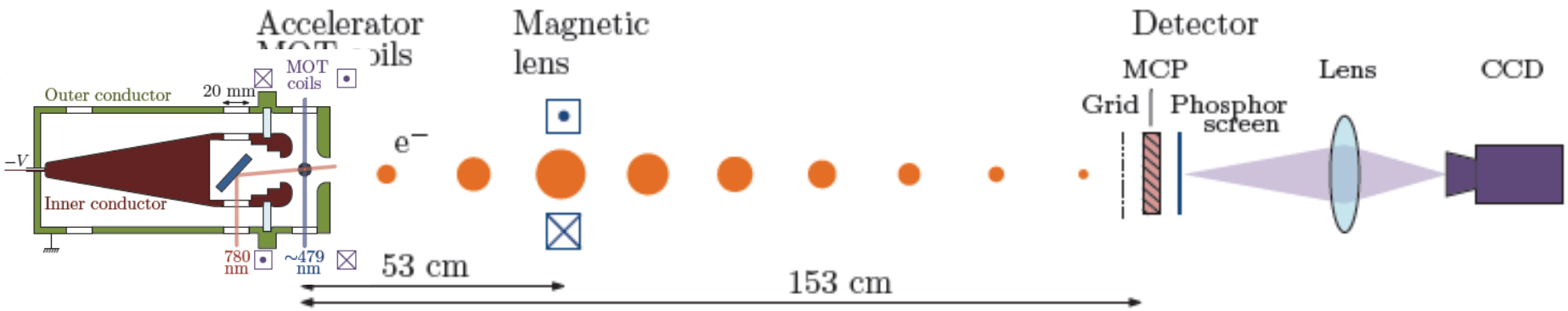

σ_{el}~20 μm controlled by ionization laser
Energy measured with Time of Flight from ionization laser (photodiode) to screen
0.4 fC measured on Faraday Cup (~ 3000 particles)
MCP-phosphor screen (photo-multiplication) for enhancing signal for single electron detection
Pinhole for resolution determination ~100μm

Courtesy O.J.Luiten

Engelen et.al Nature Communications "High-coherence electron bunches produced by femtosecond"
Engelen et al "Effective temperature of an ultracold electron source based on near-threshold Photoionization"

Solenoid scan
for an extremely small emittance

Transverse emittance , low energy
Destructive
Multi Shot

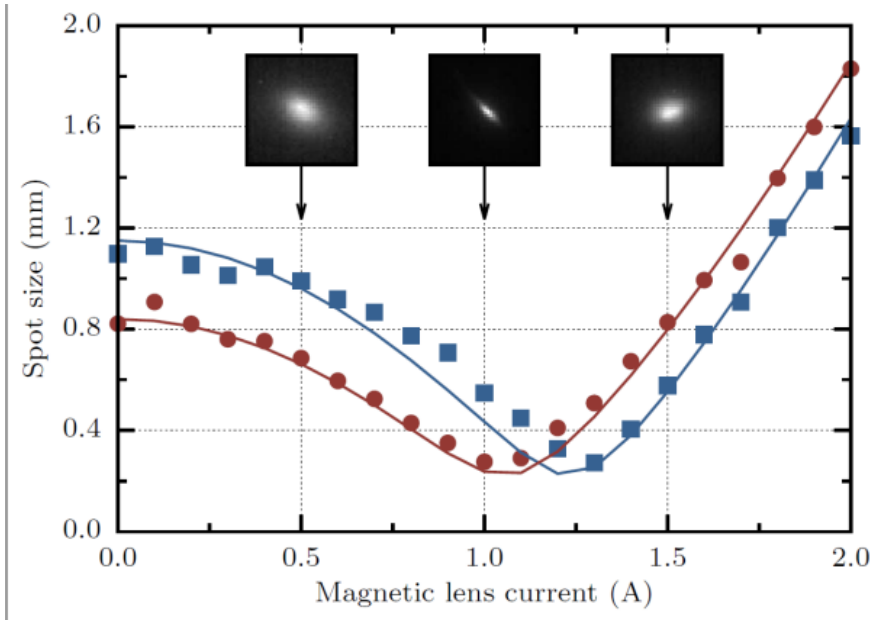

Courtesy O.J.Luiten

$\varepsilon = 1.4nm$ for Q =0.5 fC (~3000 particles)
Equivalent to 70 nm-rad per mm rms
~ 10 times smaller than RF photoinjectors
So 100 times larger brightness

Main conclusion
fs-ionization still allows to reach 20K thermal emittance

Engelen et.al Nature Communications “High-coherence electron bunches produced by femtosecond”
Engelen et al “Effective temperature of an ultracold electron source based on near-threshold Photoionization” Ultramicroscopy

Spatial projection : choice of “screens”

Very good physics description of physics E.Bravin in
http://cds.cern.ch/record/1071486/files/cern-2009-005.pdf

Screens

ZnS phosphor screens

- small dynamic range , easily saturated
- grain size ~ 20μm
- response time

YAG screens :

- good yield
- thickness
- response time

Scintillator properties : http://scintillator.lbl.gov/

YAG combined with MCP for low electron density

OTR screen

Wire scanner

Ultimate wire

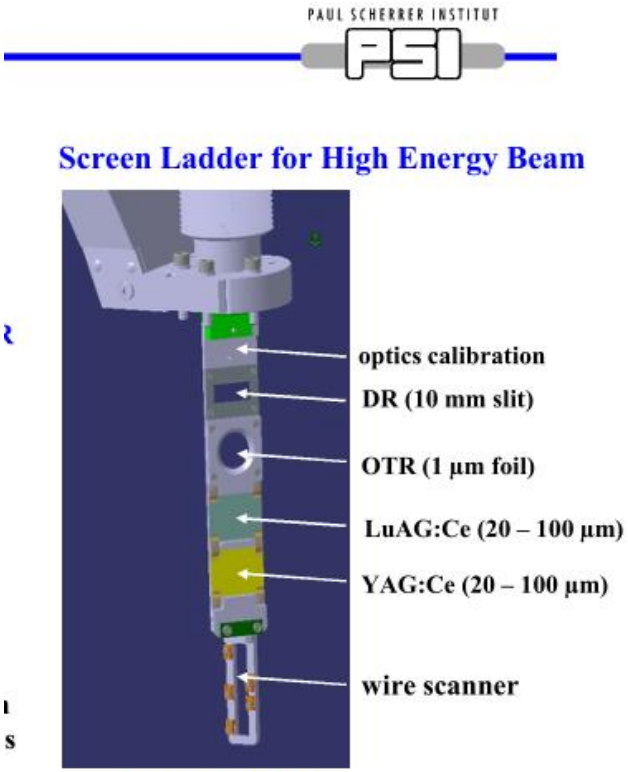

Courtesy of AMI

OTR (Optical Transition Radiation)

- Emitted when a relativistic electron passes boundary between materials of different electrical properties

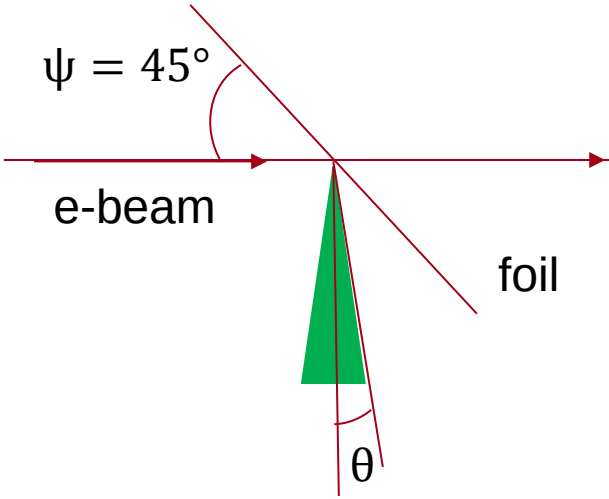

- OTR emission from a single electron
  - Travelling with relativistic velocity $\beta \approx 1 - \frac{1}{2\gamma^2}$
  - Hitting a foil with reflectivity $R(\omega)$ foil
  - Typically at 45 degrees w.r.t to beam direction

- $$\frac{d^2N}{d\omega d\Omega} = \frac{\alpha}{4\pi^2}\frac{R(\omega)}{\omega}\frac{\beta^2 sin^2(\theta)}{\left(1-\beta cos(\theta)\right)^2}$$

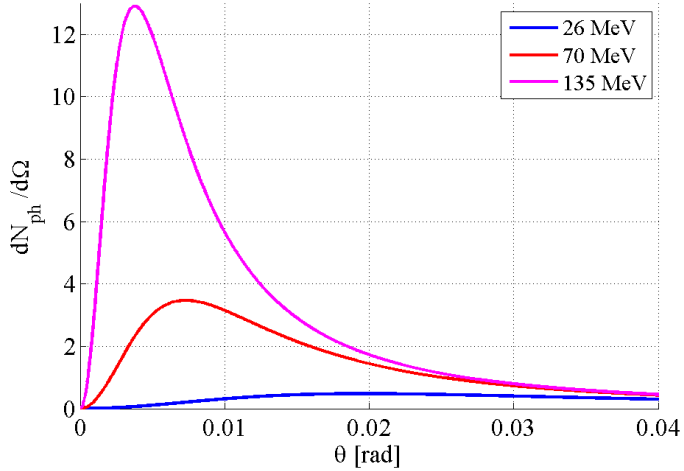

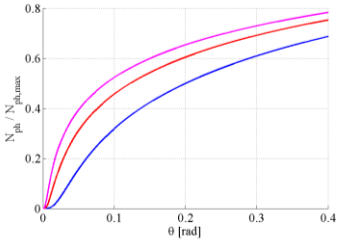

$\theta > 150\ mrad$,
$60\%\ of\ light$

OTR far-field imaging

Can we do far-field imaging and obtain the e-beam divergence ?

Deconvolution of e-beam divergence with single e angular distribution

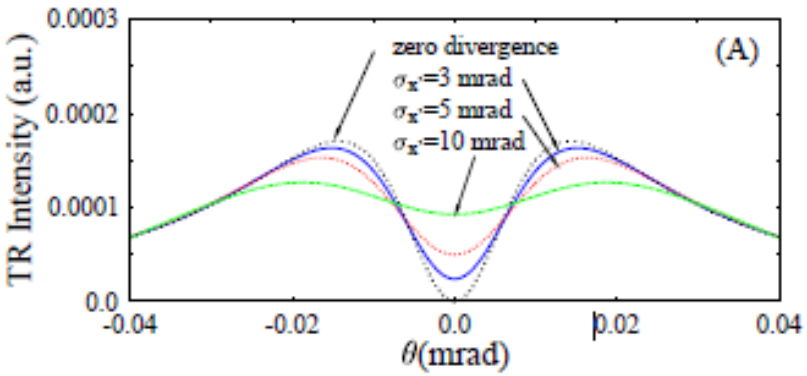

resolution $x' \sim \frac{0.15}{\gamma}$

(too poor for high brightness beams)

but accurate energy measurement

OTR interferometry

Back TR from 1st foil

Distance between 2 foils > $\lambda\gamma^2$

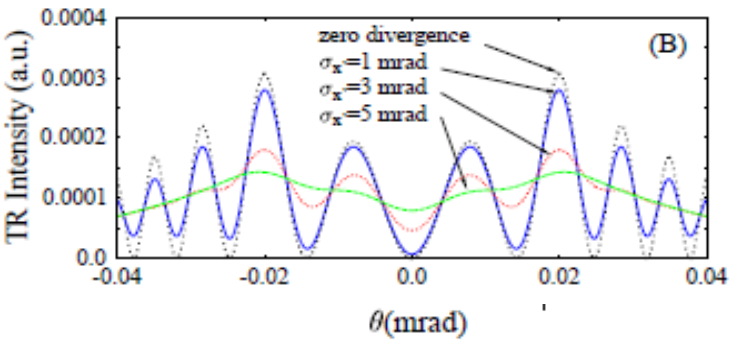

resolution $x' \sim \frac{0.075}{\gamma}$

Simulations P.Piot , 38 MeV

R.Fiorito OTR-ODR interferometry $x' \sim \frac{0.02}{\gamma}$

OTR (Optical Transition Radiation)

- Calculate $N_{photons}$
  - Spectral reflectivity of foil (Al,Ti, Be,Si)
  - Spectral sensitivity of imaging system (lens, CCD)
  - $S(\lambda_i, \lambda_f) = \int_{\omega_i}^{\omega_f} \frac{R(\omega)}{\omega} S(\omega) d\omega$

$$\int_{\omega_i}^{\omega_f} \frac{R(\omega)}{\omega} d\omega = [\log \omega]_{\lambda_i=400nm}^{\lambda_f=700nm} = 0.56$$

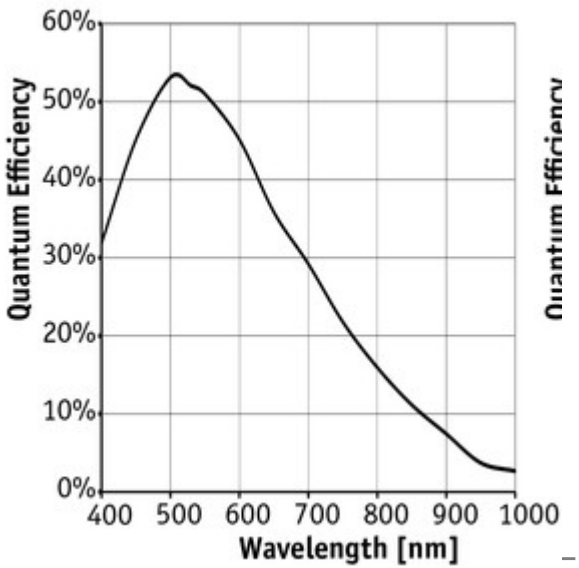

Quantum Efficiency from Sony ICX445

Imaging using OTR light

Beam size : “point-to-point imaging”

Point Spread Function (PSF) : single e emission (Green’s) through imaging system

$PSF * \rho(x, y)$ (for incoherent emission)

Example:

50 μm, 1:1 imaging ,100pC , 70 MeV

Collection angle = 100mrad

BW=0.7, QE = 0.5

$N_{electrons}$ ~2.10^6

Disk with 1.5 rms contains 70% of particles

With pixel size (3.75 μm)2 , ~ 1000 e per pixel

NB: full well capacity 30000,

With 8 bits above noise => noise level at 100e

~ 10 pC

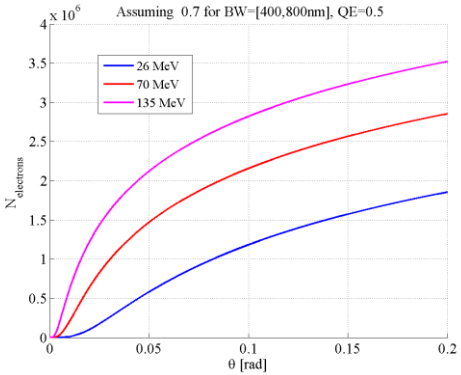

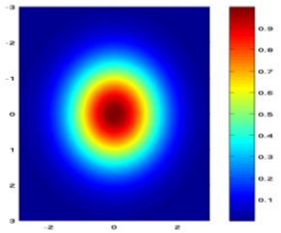

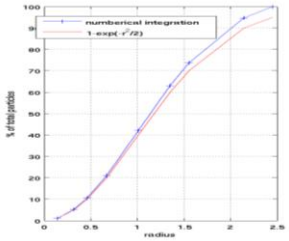

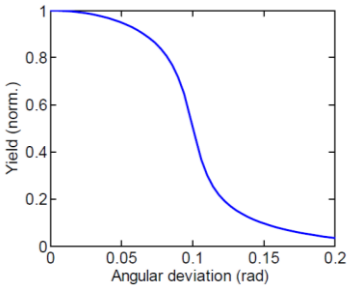

Tight Alignment tolerances

OTR (Optical Transition Radiation)

- PSF "Point Spread Function": response of imaging system to a point source

- Incoherent: $Image(O_1 + O_2) = Image(O_1) + Image(O_2)$
  $PSF * \rho(x, y)$ => $intensity \propto N_e$

- Coherent: image formation linear in complex field
  In short $FT^{-1}\left(E_s(k_x, k_y) \times \rho(k_x, k_y)\right)$

$\boldsymbol{E}(\boldsymbol{r}) = \frac{q}{\pi v}\frac{\boldsymbol{r}}{r}\alpha K_1(\alpha r)$ electric field at the transition radiation source with $\alpha = \frac{k}{\beta\gamma}$

$$E_{S,N}(r) = \sum_j e^{-jkz_j}\, E_s\left(r - r_j\right)$$

$$\left|\boldsymbol{E}_{S,N}(\boldsymbol{r})\right|^2 = N \int d^2 r'\, dz\;\; \rho(\boldsymbol{r}', z)\left|\boldsymbol{E}_{S,N}(\boldsymbol{r} - \boldsymbol{r}')\right|^2$$

$$+ N^2\left|\int d^2 r' dz\;\; e^{-ikz}\, \rho(\boldsymbol{r}', z)\boldsymbol{E}_{S,N}(\boldsymbol{r} - \boldsymbol{r}')\right|^2$$

- Microbunching generates phase relations for particles along bunch making the N2 component large and dominant

Coherent OTR (COTR)

Coherent emission:

OTR image show square of gradient of shape
thus the “doughnut” shape

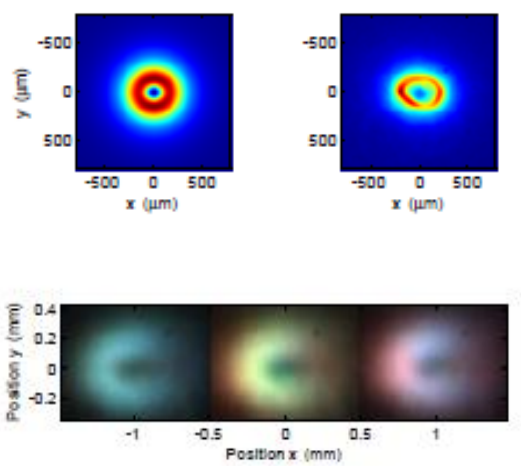

Figure 10: Series of COTR color images taken within one minute showing varying color content from shot to shot.

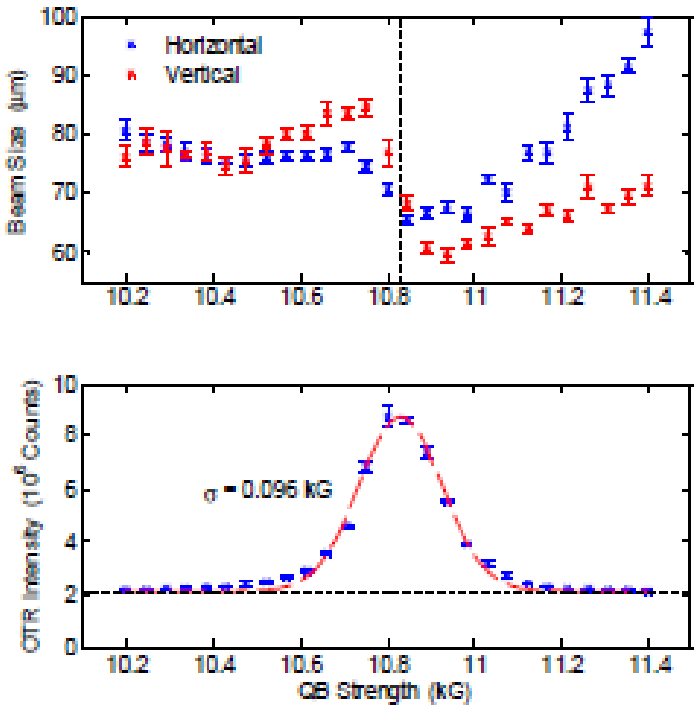

Spoils measurement of rms beam size (under estimate)
Starts from shot noise => present in continuous spectrum

OTR for beam size measurement

COTR suppression:

Smearing out microbunching

Spectral separation: imaging for $\lambda < \lambda c$ (ie extreme UV, in vacuum)

Spatial separation: Use scintillator screen , tilted to avoid COTR

Temporal separation: (scintillator response ~ 70 ns) with expensive ICCD

Use Phase retrieval algorithm (A.Marinelli) on far-field COTR

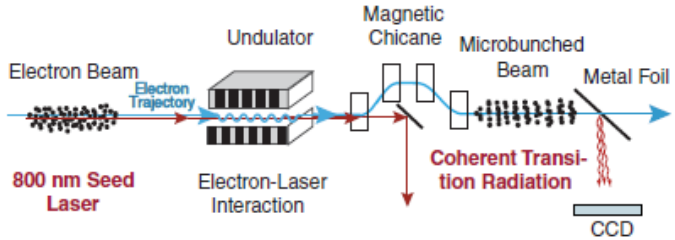

Beam size measurement despite COTR

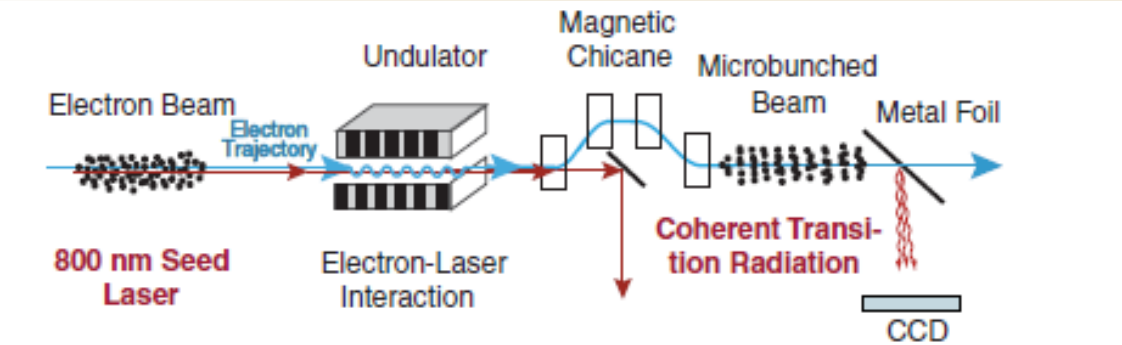

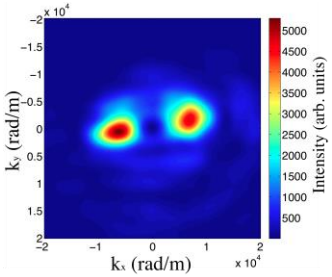

Far Field
COTR

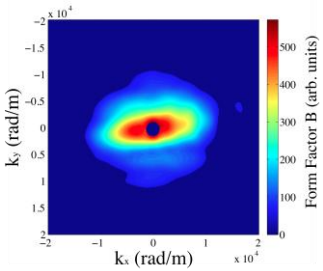

$|B(k_x,k_y)|$

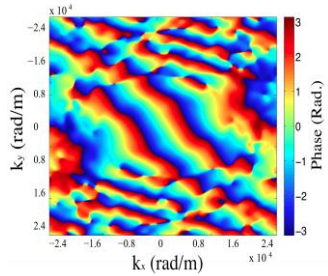

Phase$\{B(k_x,k_y)\}$

A,Marinelli et al .
PRL 110, 094802 (2013)

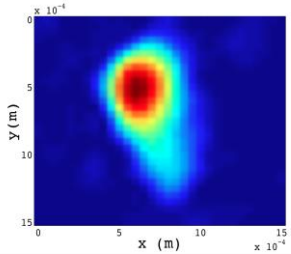

Reconstructed image
(beam is micro-bunched)

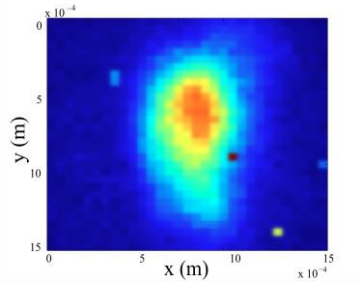

No-microbunching
Direct OTR imaging

Wire scanner

Non-destructive beam size
Multi Shot

Small wire intercepts beam

Bremsstrahlung radiation and scattered electrons detected on fast ion chambers with PMTs (PMT = Photo-Multiplying tubes)

detecting Cerenkov from secondary electrons

light from plastic scintillator fibers along chamber

Positioned at low background location

Material

W more signal but burn more easily ~ 20-40 μm

C less signal , but more robust can go down to few μm

for a 4 μm rms beam sizes down to 1 μm can be measured

Major issues

break (high rep. rate and high Ipeak) 2nC in wire of 1 μm

vibrations

beam jitter (from magnet power supplies stability)

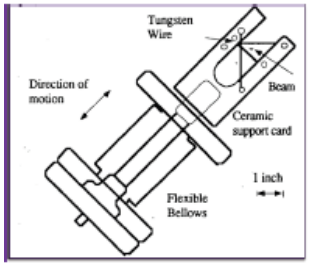

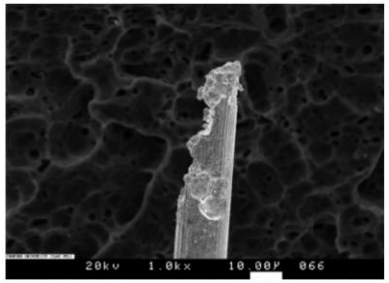

FIGURE 3. Failed 15 μm diameter tungsten wire showing the rough surface resulting from many discharges.

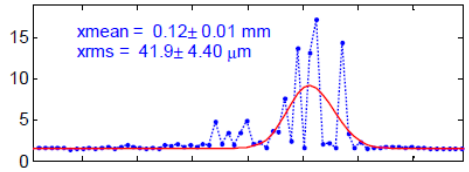

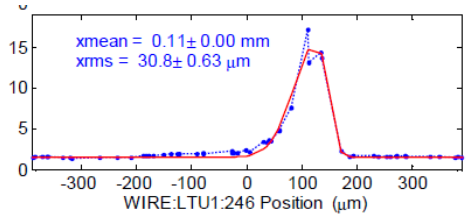

Figure 4: Beam jitter correction for wire scan data. The top part shows the PMT signal vs. the raw wire position with an rms beam size of 42 μm. In the bottom part the wire position is corrected shot by shot and the rms beam size reduces to 31 μm.

H.Loos , MOIANB01 Proceedings of BIW10, Santa Fe, New Mexico, US

Wire scanner

Non-destructive beam size
Multi Shot

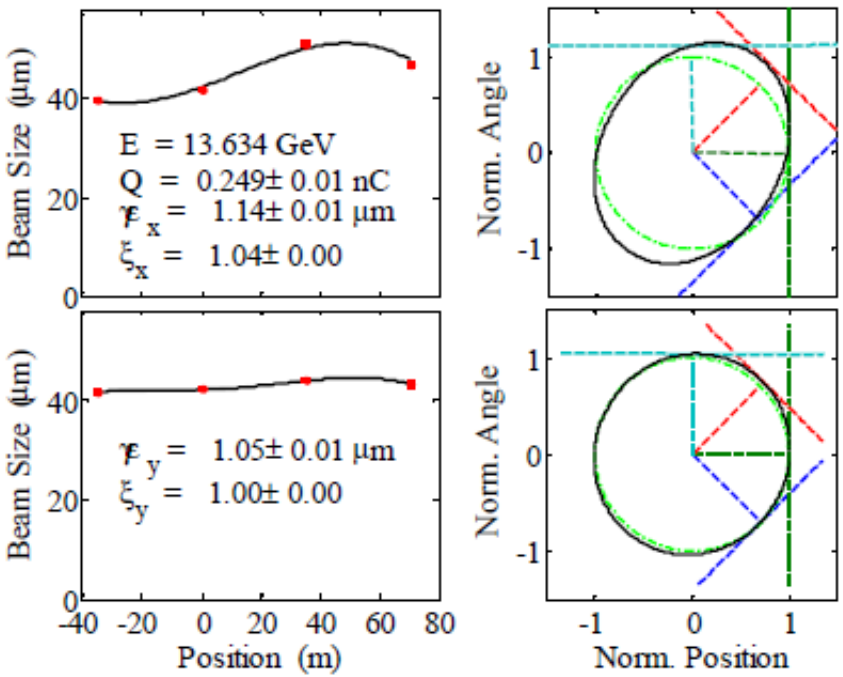

Figure 5: Emittance measurement upstream of the undulator using 4 wire scanners with 45° phase advance between them. The left panels show the measured beam sizes in the horizontal and vertical plane, and the right panels the respective normalized phase space ellipse. The dashed lines indicate the projection angle for each measurement.

H.Loos , MOIANB01 Proceedings of BIW10, Santa Fe, New Mexico, US

- Vibrations are a limitation
  resonance studies : speed tests
  optical measurements

SLAC PUB-6015 McCormick, M.Ross

Mechanical improvements to reduce further

Compton scattering process

Collision photons with relativistic electrons

Scattered photons

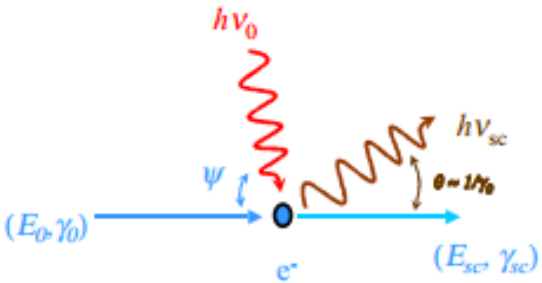

- Direction : in cone with opening angle in $1/\gamma_o$

- Frequency : Doppler shifted

$$h\nu_{sc} = h\nu_o \left(\frac{\gamma_o E_o (1-\beta_o cos(\psi))}{\gamma_o E_o (1-\beta_o cos(\psi)) + h\nu_o (1-cos(\psi-\theta))} \right) \cong 2\gamma_o^2 h\nu_o \quad \text{for } \psi \approx \frac{\pi}{2}$$

- Intensity :

$$N_{sc} \approx \sigma_c \langle n_o \rangle N_{electrons} D \qquad with\ \langle n_o \rangle = \frac{1}{h\nu_o} \frac{P}{c\,S}$$

(P, S) : ($power, spot\ size$) $of\ laser$

D : $distance\ of\ interaction$

σ_c : $Compton\ cross\ section\ \approx 6.6\ 10^{-29} m^2$

Laser wire scanner

Non-destructive
Non-degradable
Multi Shot

- measure e-beam sizes > 200nm,
- high current beams
(“non-degradable” wire)
- detection of X-Ray (or γ-rays)
or recoil energy (for very high $E_{e\text{-beam}}$)
- scan either laser or e-beam position
- detection requires bending magnet
- challenges
  synchronization
  focus
  scan

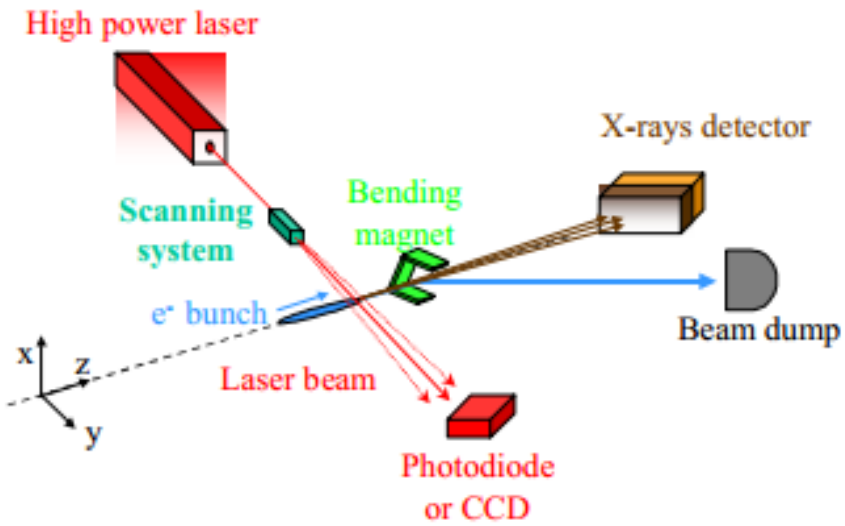

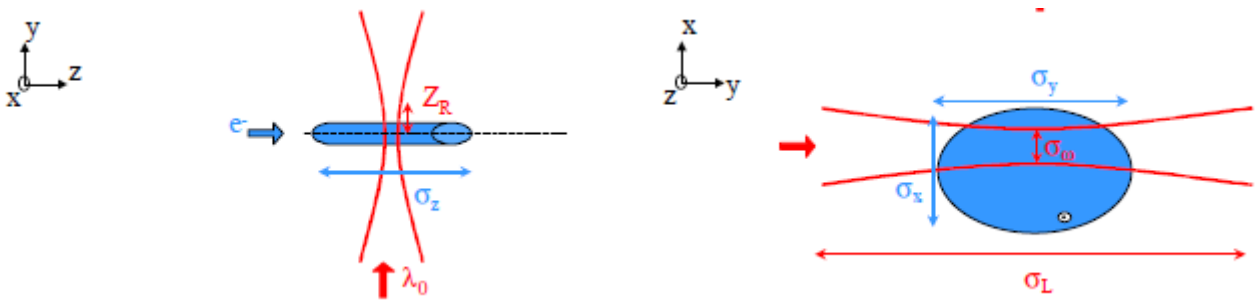

Laser wire scanner

Non-destructive
Non-degradable
Multi Shot

- Measurements SLC (pioneering experiment)

E = 45 GeV,

$N_{photons}$ at waist ~ 8000

Bunch size measured ~ 1μm

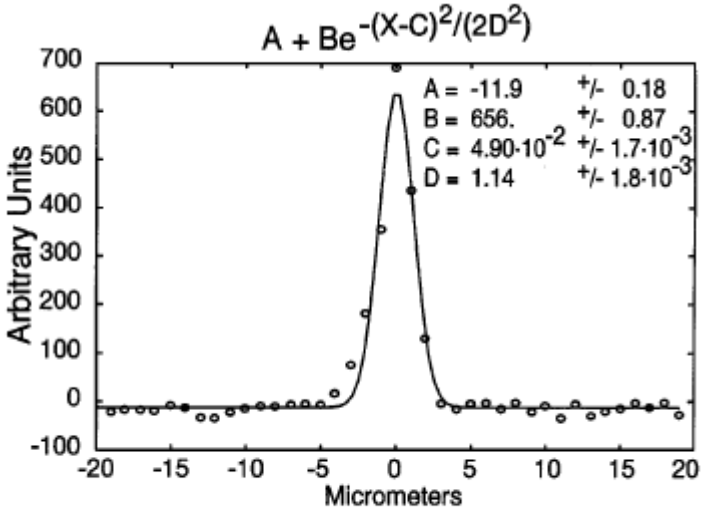

Figure 11 Measurement of the beam transverse size with a laser wire. The measured beam size is approximately 1 μm.

Laser wire scanner

Non-destructive
Non-degradable
Multi Shot

- Focus:

  Diffraction limit of a laser beam $\sigma_f = \frac{\lambda\ f}{4\pi\sigma_{laser,ini}}$

  Rayleigh length $z_r = \frac{4\pi\sigma_f^2}{\lambda}$

  Example: σ_f ~125nm , z_r ~ 625 nm for λ = 300nm

➔ Beam size measurements limited to ~ 200nm

Applications : ERL, linear colliders

Other application: bunch length measurement

References:
Shintake, Tennenbaum , Annu. Rev. Nucl. Part. Sci. 1999. 49:125–62
Lefebvre https://cds.cern.ch/record/535808/files/open-2002-010.pdf
A.Murohk, IPAC10 “A 10 MHZ Pulsed Laser Wire scanner for energy recovery linacs”

Beam size from laser interferometer

Non-destructive
Non-degradable
Multi Shot

- measure e-beam sizes < 200nm, by beating the diffraction limit using interferences

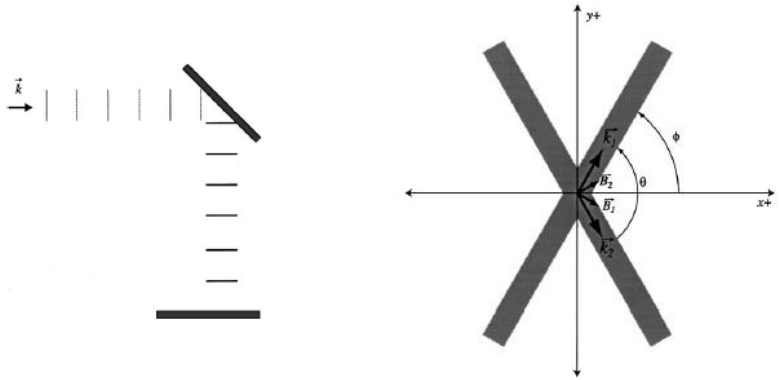

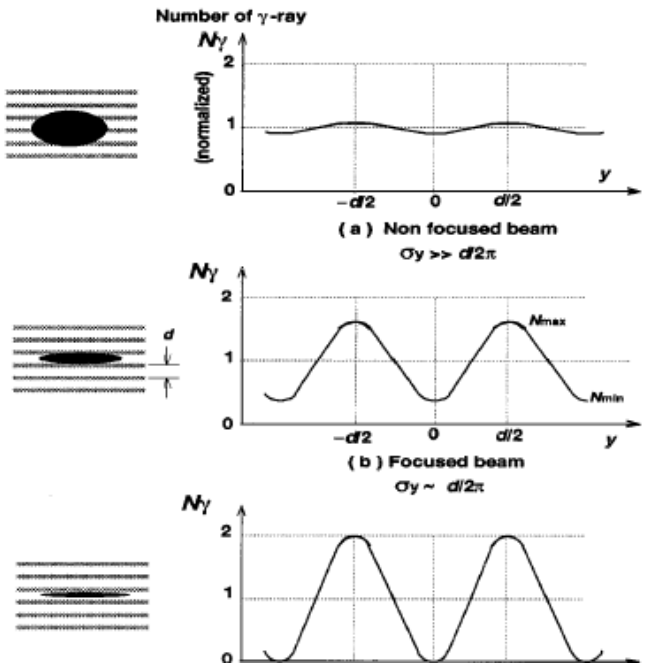

- $\langle N_\gamma \rangle = A + B\, cos(2k_L x + \psi)$
- $N_\gamma(y_o) = \frac{N_o}{2}\left(1 + cos(2k_L y_o) cos(\theta) \exp^{\left[-2(k_y \sigma_y)^2\right]}\right)$
- $N_\pm = \frac{N_o}{2}\left(1 \pm cos(\theta) \exp^{\left[-2(k_y \sigma_y)^2\right]}\right)$
- $M = \frac{N_+ - N_-}{N_+ + N_-}$
- $\sigma_y = \frac{d}{2\pi}\sqrt{2ln\left(\frac{|cos\theta|}{M}\right)}$

With $\theta = 174°$, σ_y down to 38 nm can be measured with a 1μm laser

"Shintake-monitor"

Beam size from laser interferometer

Non-destructive
Non-degradable
Multi Shot

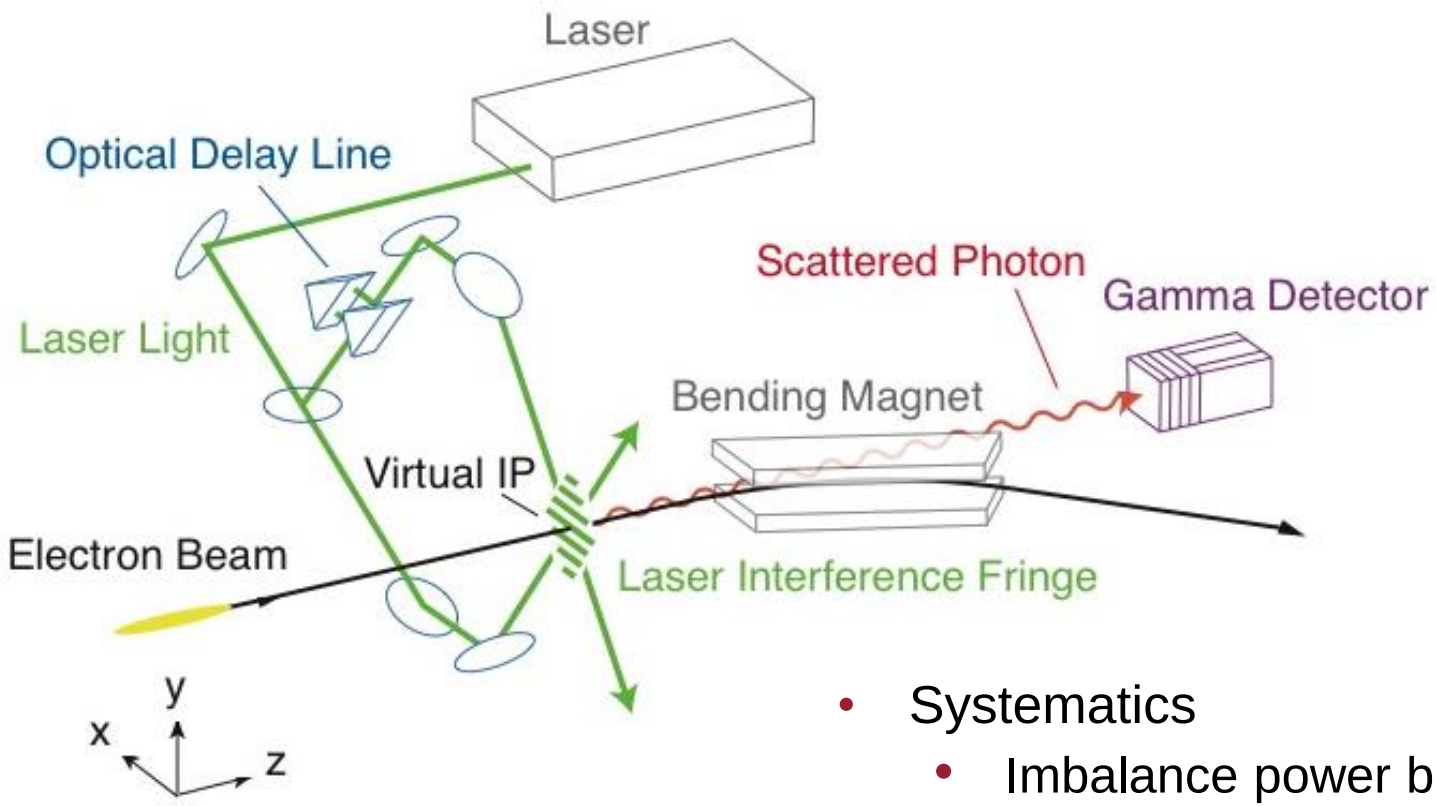

- Systematics
  - Imbalance power between 2 arms
  - Variation in e-beam angle
  - Longitudinal extent of diffraction pattern
  - Spherical wavefront error
  - Coherence of laser (transverse + longitudinal)

Courtesy Jacqueline Yan,KEK

Beam size from laser interferometer

Non-destructive
Non-degradable
Multi Shot

- Shintake pioneering measurement SLAC (1994)

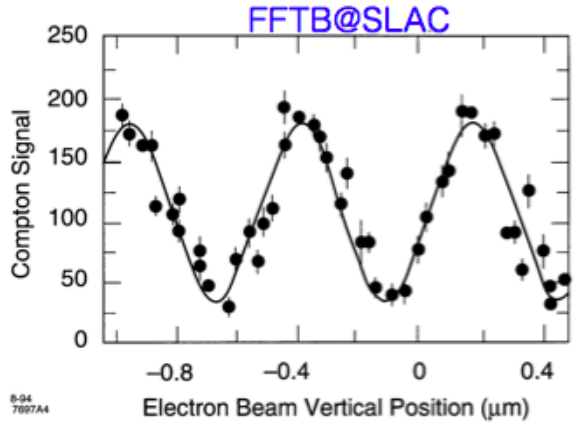

E = 46.6 GeV
$\sigma_y \sim 77$ nm

T.Shintake, P.Tenenbaum, Annu. Rev. Nucl. Part. Sci. 1999. 49:125–62
http://www.jlab.org/accel/beam_diag/DOCS/annurev.nucl.49.1.125.pdf

- KEK measurements

1.6nC

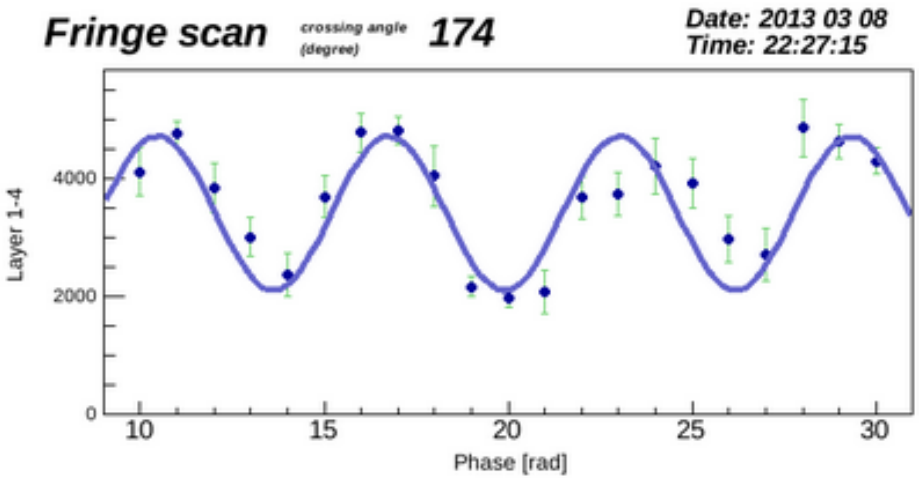

1.3 GeV, $\theta = 174°$
Very reproducible over 20 minutes
M ~ 0.306 ie $\sigma_y \sim 65$ nm
Best measurement $\sigma_y \sim 58$ nm

Goal = 37 nm

Courtesy Jacqueline Yan,KEK,

Optical Diffraction Radiation Interferometry (ODRI)

Non-destructive
For single shot x,x'

- 0.4nC * 20 bunches at 5Hz ~ 80nC enough to damage OTR
- 2 apertures at d < $\lambda\gamma^2$ ("formation length") but with different aperture size

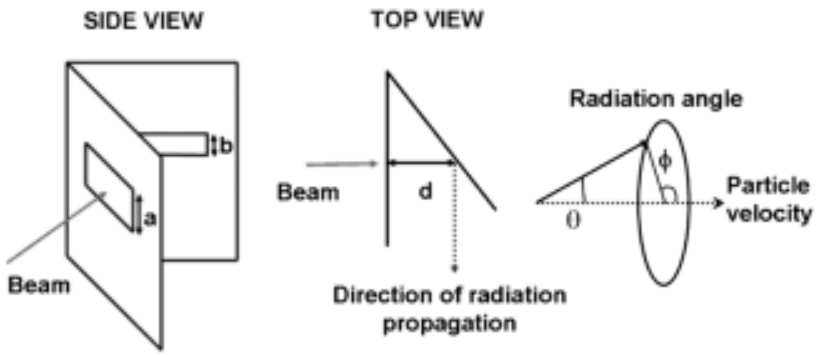

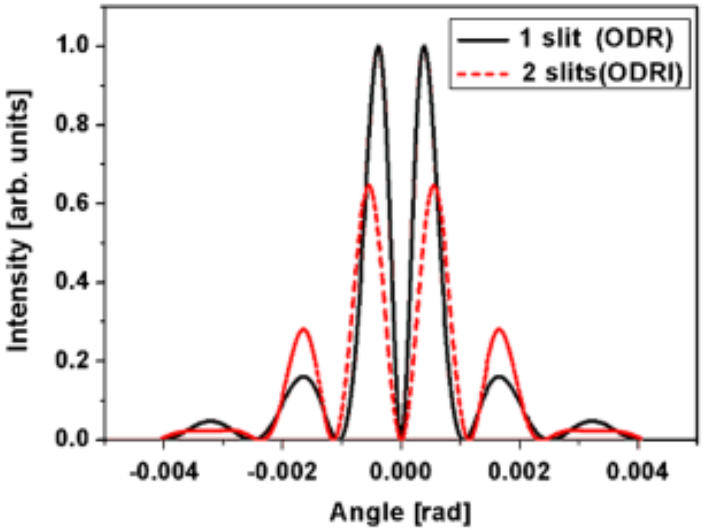

A.Cianchi Journal of Physics: Conference Series **357** (2012) 012019
http://prst-ab.aps.org/pdf/PRSTAB/v14/i10/e102803

Optical Diffraction Radiation Interferometry (ODRI)

Non-destructive
For single shot x,x'

- Calculation

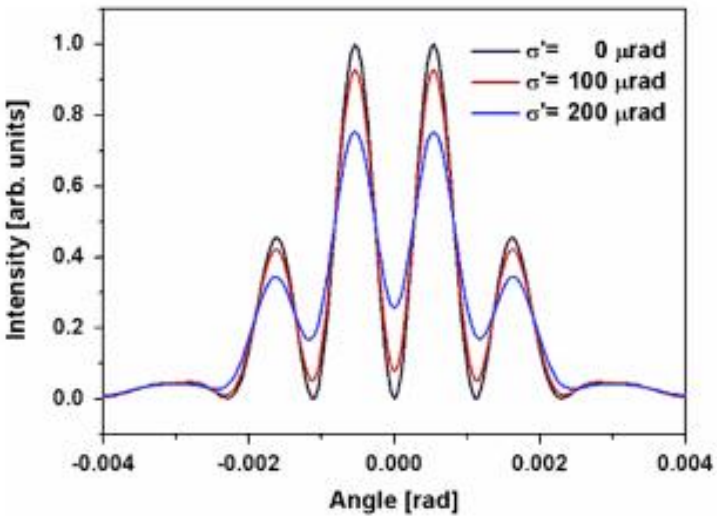

Measurements

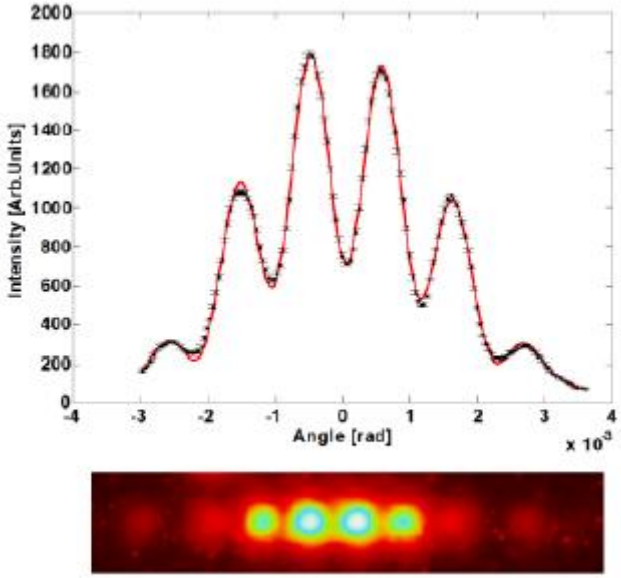

$$\sigma_y = 81\mu m, \sigma_{y'} = 203\ \mu rad$$

A.Cianchi Journal of Physics: Conference Series **357** (2012) 012019
http://prst-ab.aps.org/pdf/PRSTAB/v14/i10/e102803

“single point” emittance measurement

Destructive or non-destructive Single Point

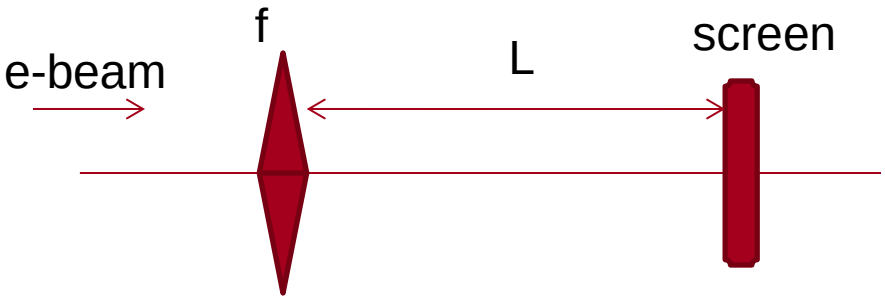

$$\begin{cases} x = \left(1 - \frac{L}{f}\right) x_o + L x_o \\ x' = -\frac{x_o}{f} + x'_o \end{cases}$$

$$\langle x^2 \rangle = \left(1 - \frac{L}{f}\right)^2 \langle x_o^2 \rangle + 2L\left(1 - \frac{L}{f}\right) \langle x_o x'_o \rangle + L^2 \langle x'^2_o \rangle$$

$$\langle x x' \rangle = -\frac{1}{f}\left(1 - \frac{L}{f}\right) \langle x_o^2 \rangle + \left(1 - \frac{2L}{f}\right) \langle x_o x'_o \rangle + L \langle x'^2_o \rangle$$

Find magnet setting f* such that $\frac{\partial(\langle x^2 \rangle)}{\partial f} = 0$

then correlation term $\langle x x' \rangle = \frac{\langle x^2 \rangle}{L}$

at f* , measure $\langle x^2 \rangle$, and deduce $\langle x x' \rangle$

measure $\langle x'^2 \rangle$

➔ emittance at single point

(with 2 images : one near-field, one far-field)

BUNCH LENGTHS

Electro-Optic methods

Bunch length
Non-destructive

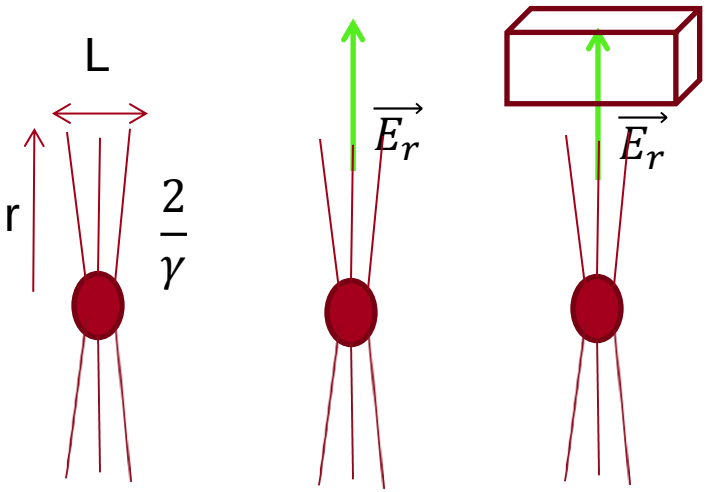

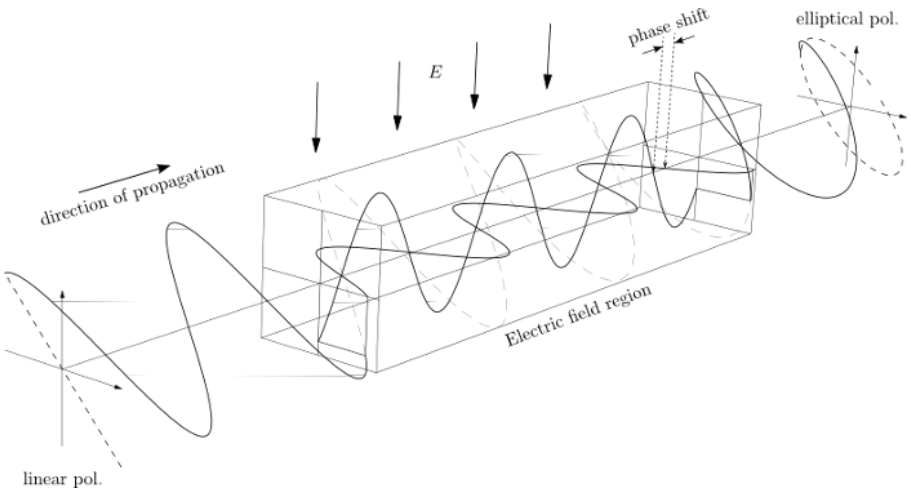

500 MeV (γ = 1000)
r = 5mm
L = 10 μm = 33 fs

$\overrightarrow{E_r}$ component of Lorentz contracted Coulomb field

Birefringence induced by $\overrightarrow{E_r}$, $P = \varepsilon_o \left(\chi_e^{(0)} E + \chi_e^{(1)} E^2 + \cdots\right)$

Pockels Kerr

Changes polarization and introduces phase retardation

As an E-field pulse mixer, casually referred to as an “ultrafast Pockels cell”

Electro-Optic Sampling

Bunch length
Non-destructive
Multi Shot

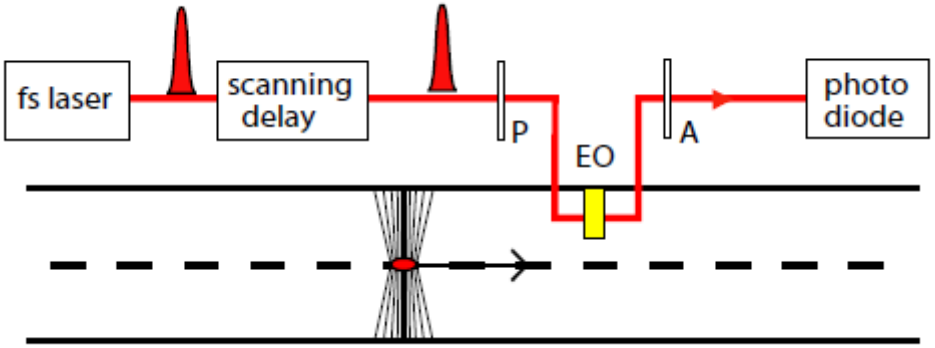

from Bernd Steffen, DESY

1. Laser pulse much shorter than e-beam pulse used as probe
   - Samples small part of e-beam field
2. Analyzer (polarizer) to transmit polarization change to photo-diode
3. Scan delay to trace out e-beam profile

Limitation as multi-shot method:

- Shot-to-shot timing jitter bad for profiling
- (Still useful time of arrival monitor)

Electro-Optic spectral decoding

Bunch length
Non-destructive
Single Shot

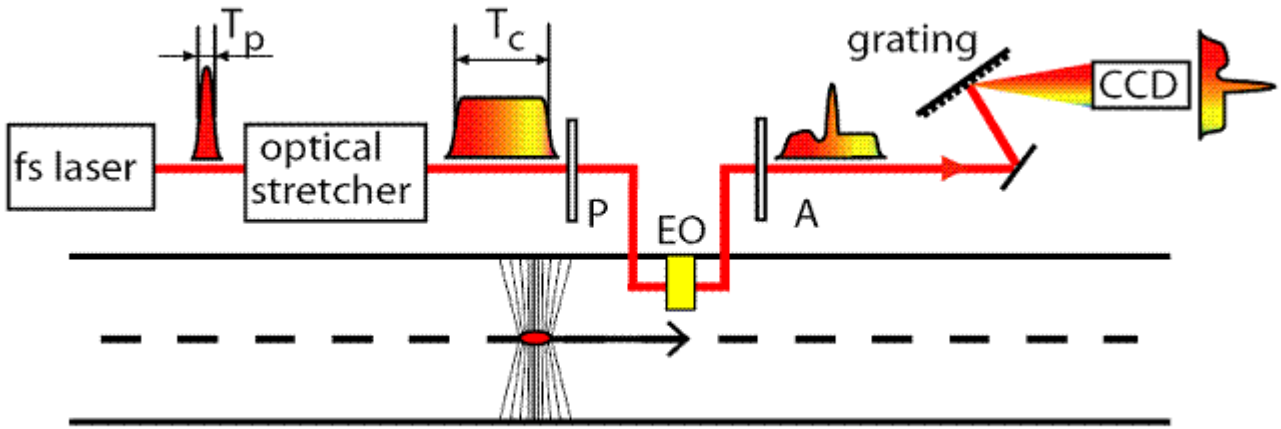

from Bernd Steffen, DESY

1. Laser pulsed stretched: long chirped laser with linear λ-t correlation
2. Interaction with E_r from e-beam in EO induces t-dep. change in polarization
3. Analyzer/spectrometer measures change in polarization as function of λ
4. Map λ back to t to deduce e-beam profile

Limitation from non-linear optical mixing:

- Resolution t_{res} worsens with increasing chirp duration "window" T_c as $t_{res} \propto \sqrt{T_p T_c}$

Typ. temporal resolution > 200fs

Electro-Optic temporal decoding

Bunch length
Non-destructive
Single Shot

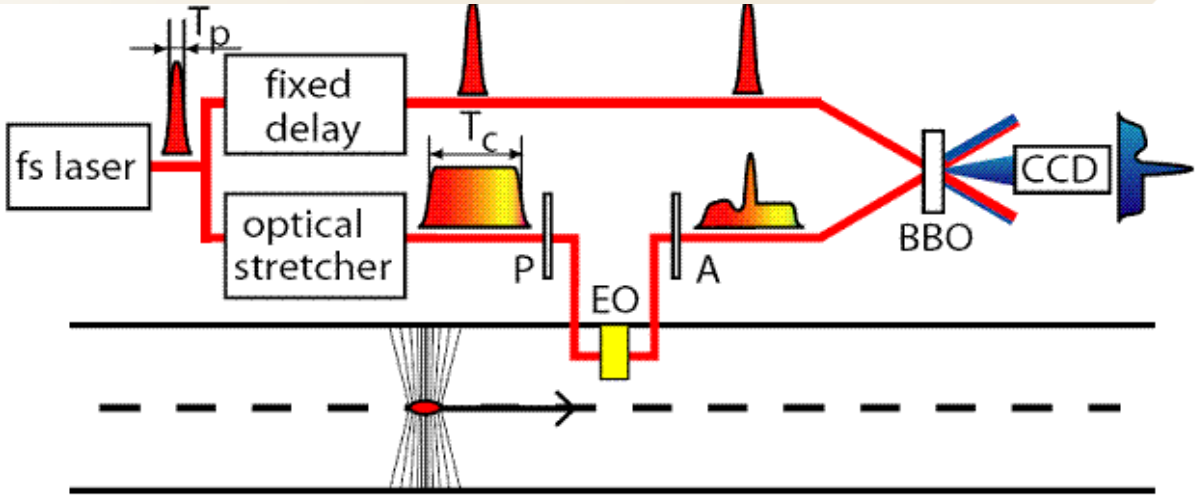

Fig. 2. Set-up for EO temporal decoding.

from Bernd Steffen, DESY

$$I_{SHG}(x) = \int I_{probe}(t+\tau) + I_{gate}(t)\, dt$$

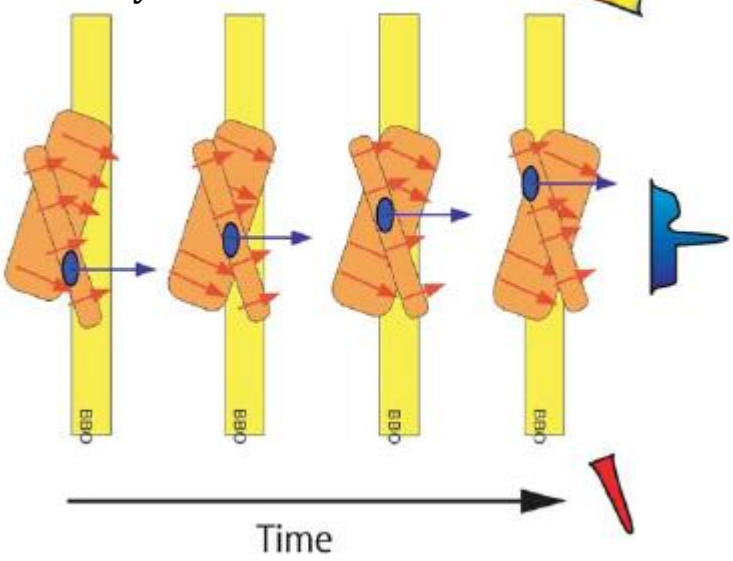

- Similar to before but pulse is decoded in time-domain
- Decoding setup similar to fast, optical cross-correlator

Limitations: again, gate width
thickness of BBO
spatial resolution

Electro-Optic temporal decoding

Bunch length
Non-destructive
Single Shot

Temporal resolution achieved ~ 60 fs
Benchmarked with transverse deflector measurements

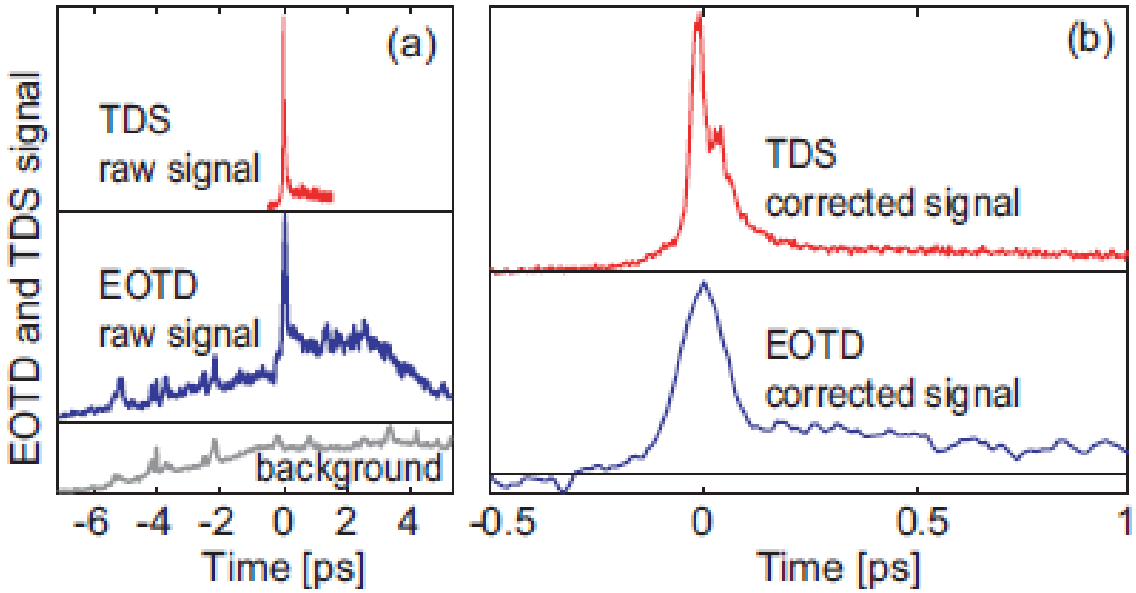

G.Berden , PRL , 99, 164801 (2007)

Electro-Optic spatially resolved

Bunch length
Single Shot

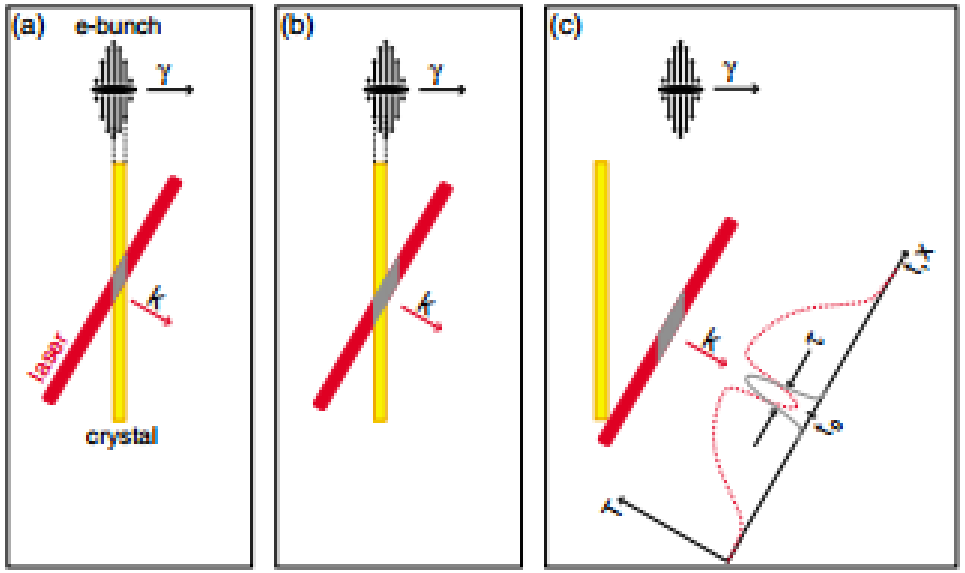

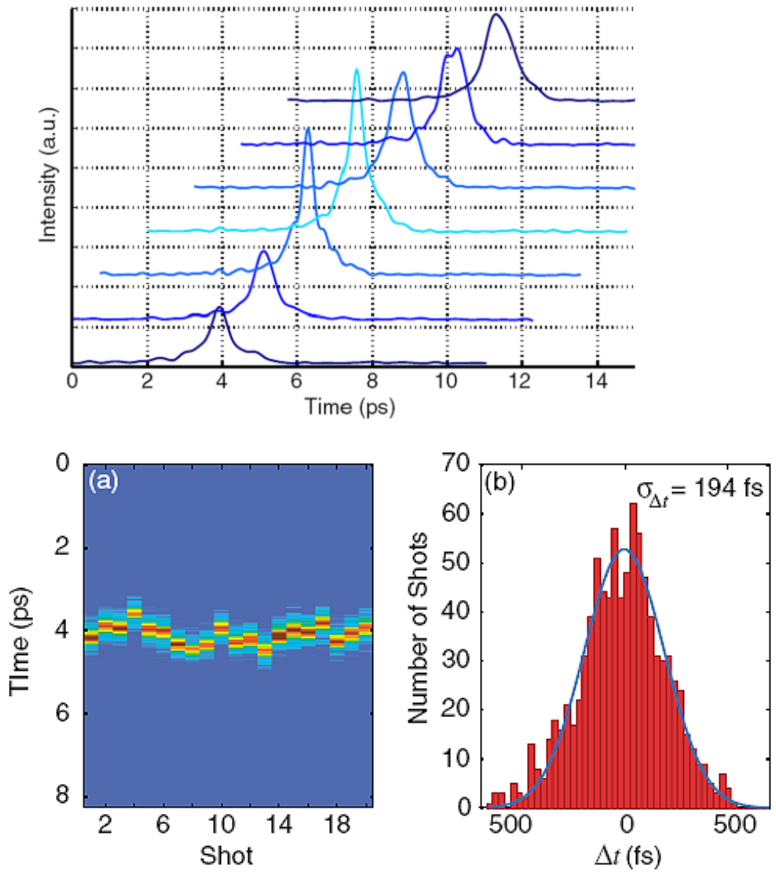

FIG. 3 (color). (a) Twenty consecutive single-shot electron bunch measurements. The bright band in each column is the electro-optic signal, its location indicates the time of arrival of the electron bunch with respect to the laser probe pulse, and its width corresponds to the electron bunch duration. (b) Normalized arrival time histogram of 1000 consecutive single shots.

A.L Cavalieri PRL 94, 114801 (2005)

Resolution ~ 115fs rms

B.Steffen PhD manuscript,
C.Casalbuoni , PRST-AB, 11, 072802 (2008)
T.Maxwell http://www.niu.edu/physics/_pdf/academic/grad/theses/Maxw

Electro-Optic limits

Bunch length
Single Shot

Maximize signal but minimize crystal size given all the broadening contributions

TO : Transverse Optical phonons limit bandwidth

GVM: Group Velocity Mismatch
(signal and probe slip through each other)

GVD : Group Velocity Dispersion
(signal and probe broaden)

Organic crystal DAST, compared to ZnTe
Both crystals are 2mm from beam , and 280 pC

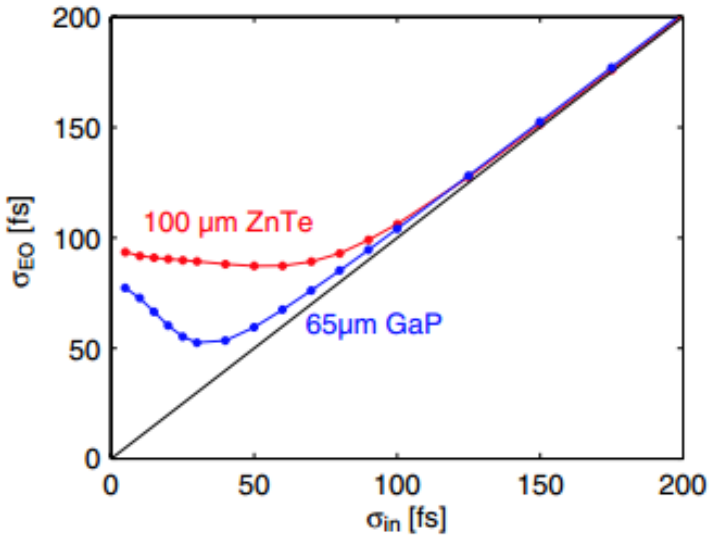

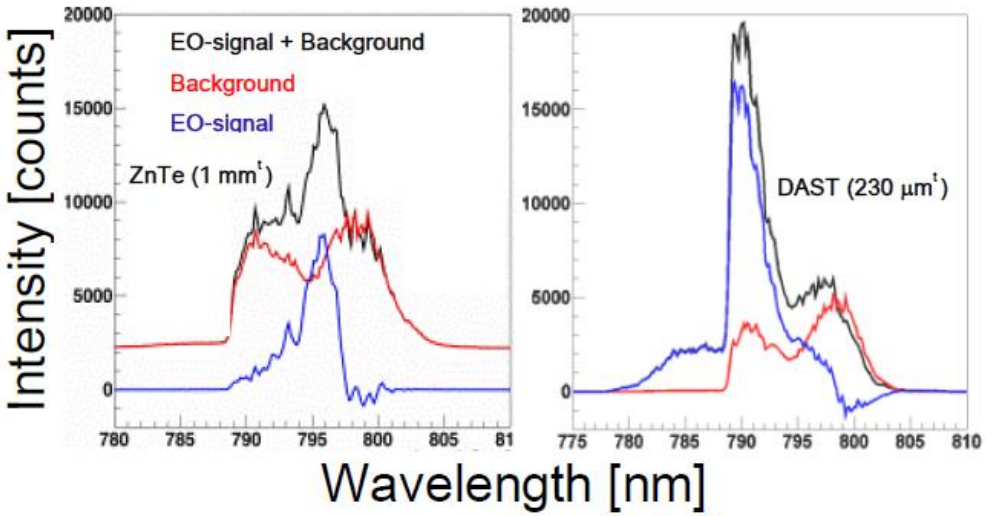

C.Casalbuoni , PRST-AB, 11, 072802 (2008)

H.Tomizawa, BIW 2012

3D –monitor Tomizawa

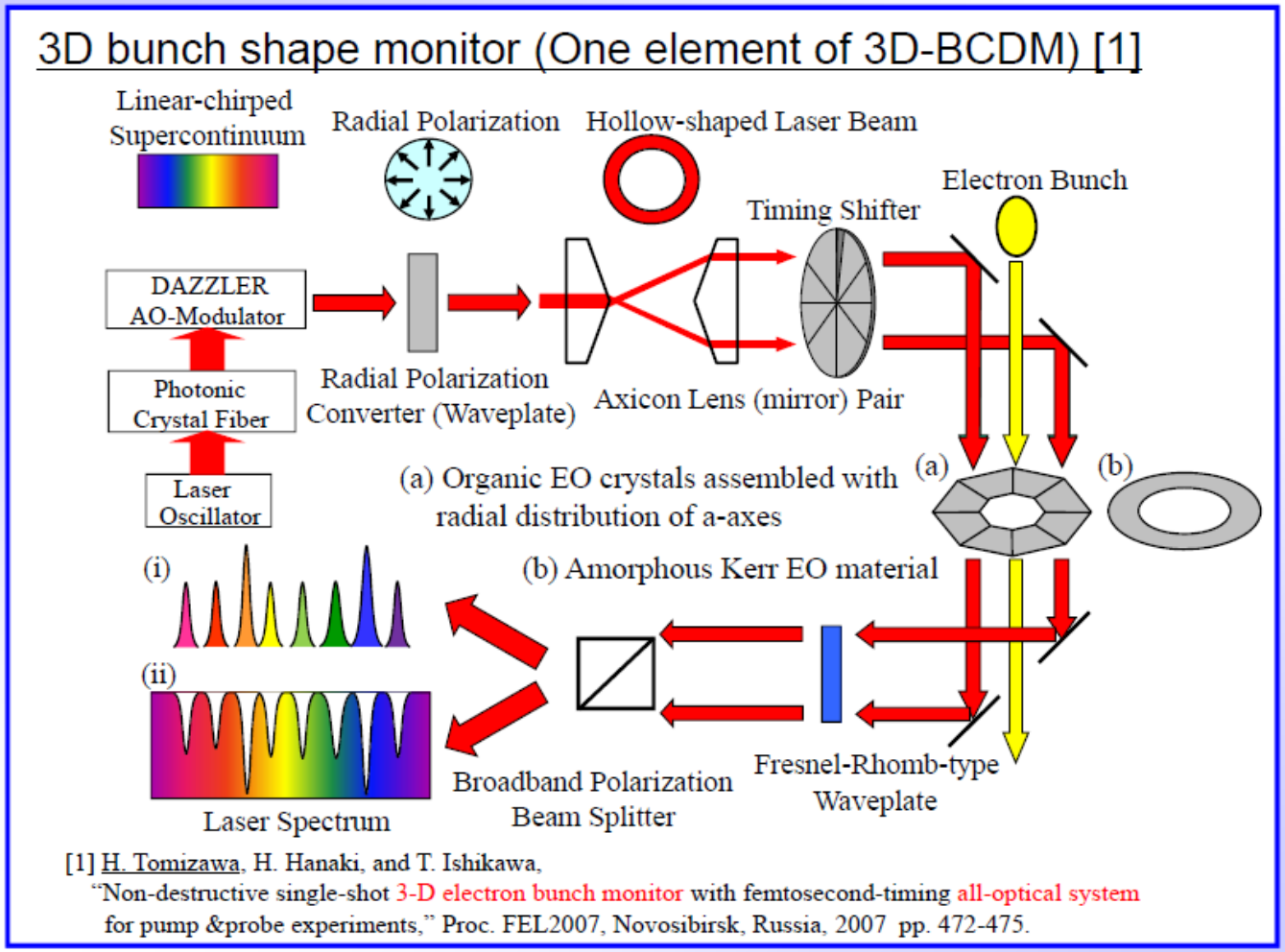

3D Monitor Tomizawa

Transverse detection (2D-charge moments *of bunch slice*)

Simulation Parameters:
Energy: 8GeV, **Charge:** 100pC, **Bunch duration:** 30fs
Detection points: 2mm from beam axis

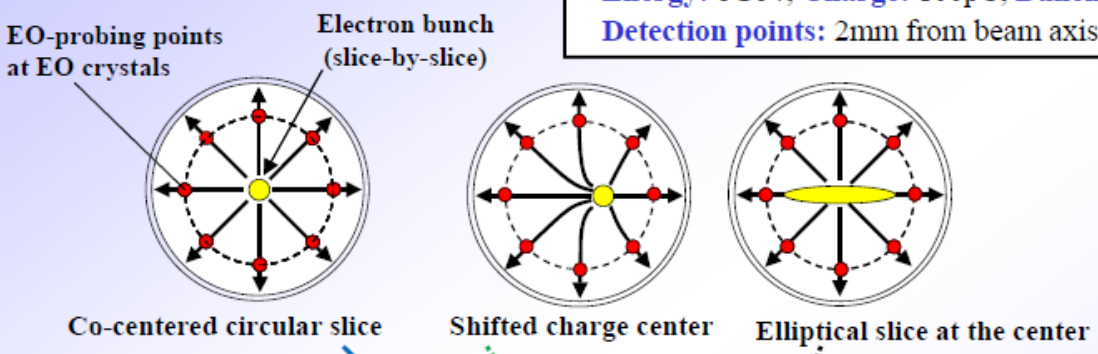

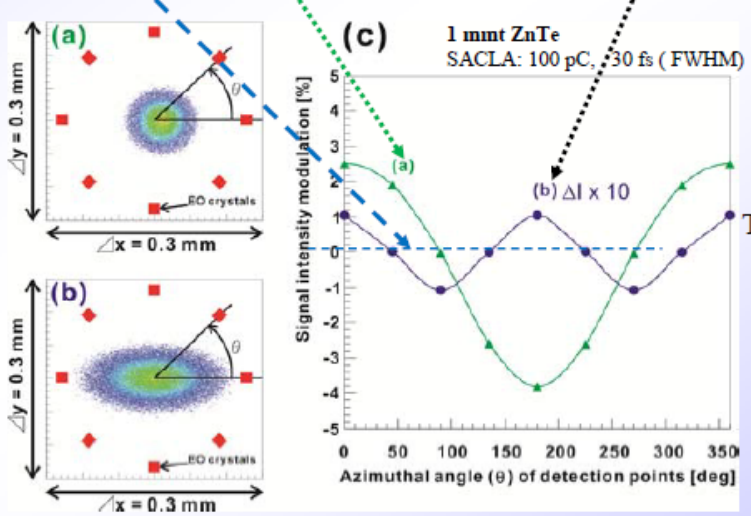

The signal intensity at the crystals

$$I = I_0 \sin^2\left(\frac{\pi}{\lambda} n_0^3 r_{41} E_r d\right)$$

Transverse deflector (TCAV)

Bunch length
Destructive
Single Shot

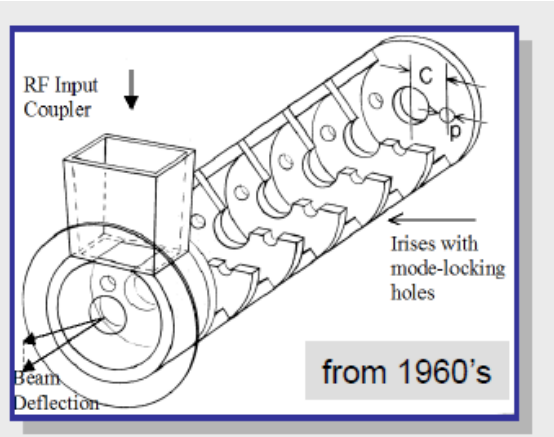

TM11 mode

$$E_r = E_0\left[\left(\tfrac{1}{2}kr\right)^2 + \left(\tfrac{1}{2}ka\right)^2\right]\cos\theta \qquad Z_0H_r = -E_0\left[\left(\tfrac{1}{2}kr\right)^2 - \left(\tfrac{1}{2}ka\right)^2 + 1\right]\sin\theta$$

$$E_\theta = E_0\left[\left(\tfrac{1}{2}kr\right)^2 - \left(\tfrac{1}{2}ka\right)^2\right]\sin\theta \qquad Z_0H_\theta = E_0\left[\left(\tfrac{1}{2}kr\right)^2 + \left(\tfrac{1}{2}ka\right)^2 - 1\right]\cos\theta$$

$$E_z = iE_0kr\cos\theta \qquad Z_0H_z = -iE_0kr\sin\theta$$

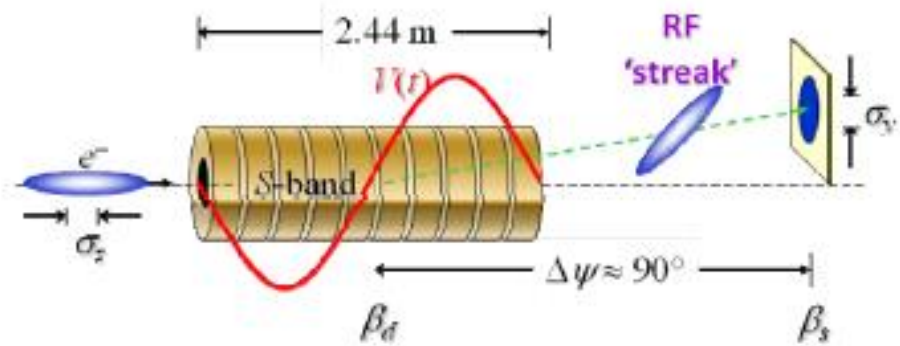

$$\Delta y'(z) = \frac{eV_o}{pc}\sin(k_{rf}z + \varphi_{rf})$$

$$\Delta y = \sqrt{\beta_{OTR}\beta_{TCAV}}\,\sin\psi_{Tcav\to OTR}\,\frac{eV_o\sin(k_{rf}z + \varphi_{rf})}{pc}$$

Resolution :

$$\sigma_y^2 = \varepsilon\beta_{OTR} + \beta_{OTR}\beta_{TCAV}\sigma_z^2\left(\frac{k_{rf}eV_o}{E}\sin\Delta\psi\right)^2$$

$$\sigma_z > \sqrt{\frac{\varepsilon}{\beta_{TCAV}}}\left(\frac{\lambda_{rf}E}{2\pi eV_o}\right)$$

Transverse deflector (TCAV)

Bunch length
Destructive
Single Shot

1- calibration at zero crossing : $1° \; RF \; to \; pixel$

$$1° \; RF \; [S - Band] = 1ps$$
$$1° \; RF \; [X - Band] = 250 \; fs$$

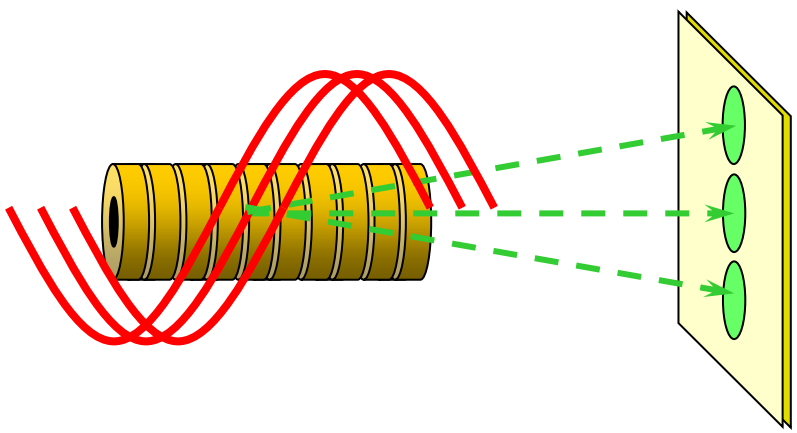

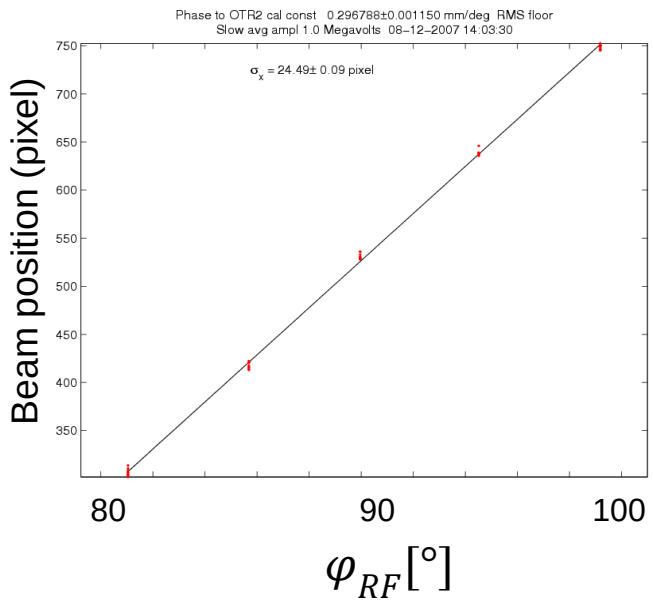

Transverse deflector (TCAV)

Bunch length
Destructive
Single Shot

Deconvolve beam size contribution

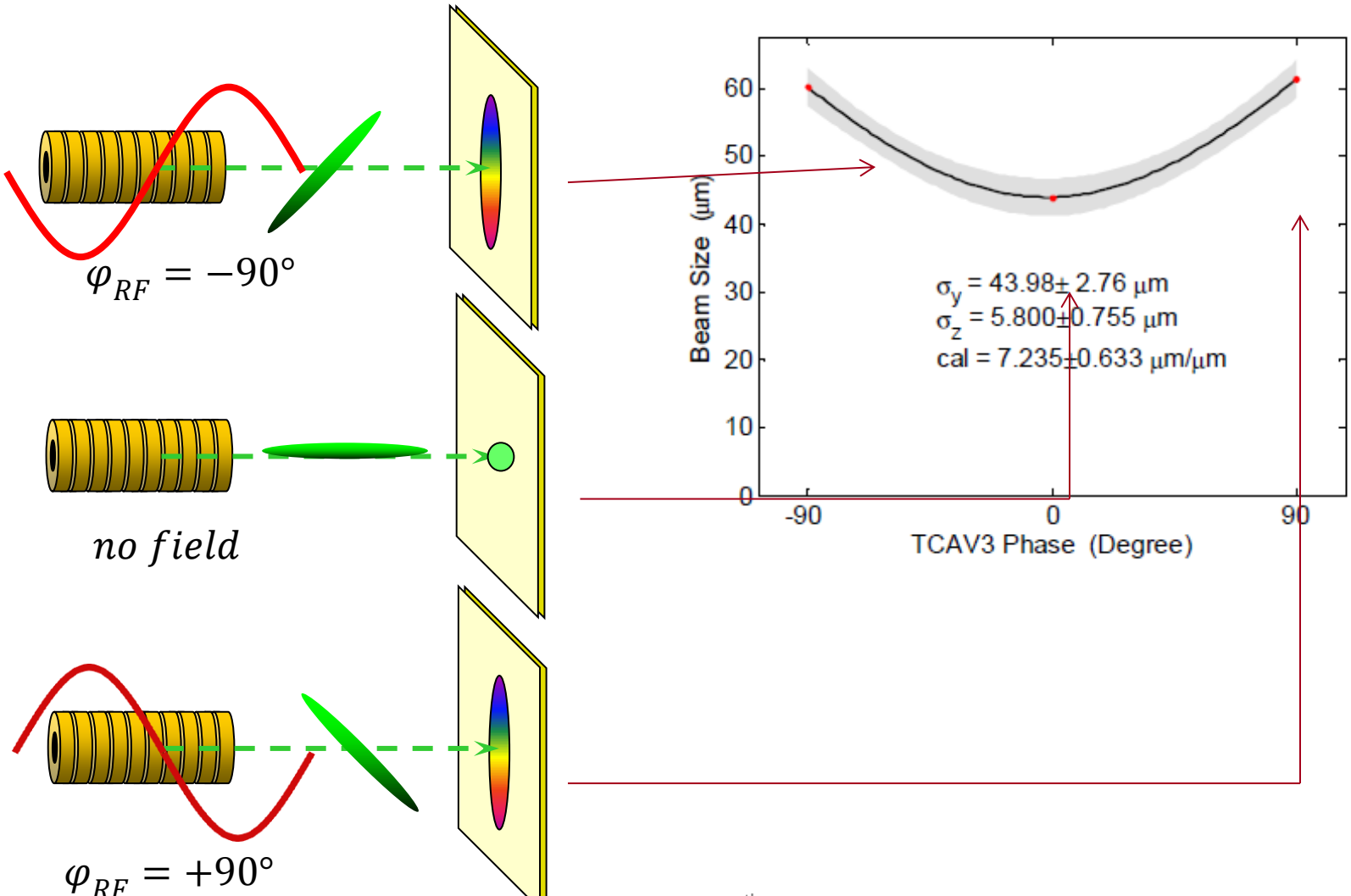

LCLS bunch length measurements

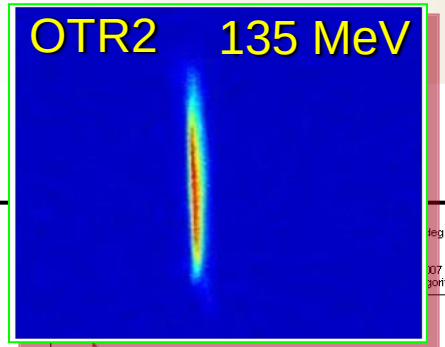

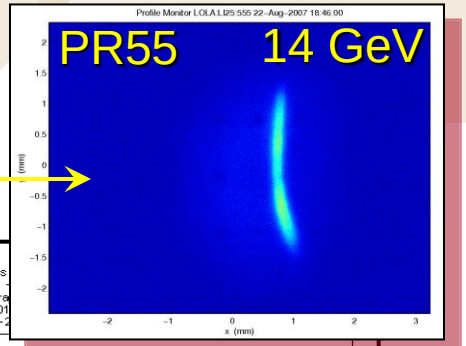

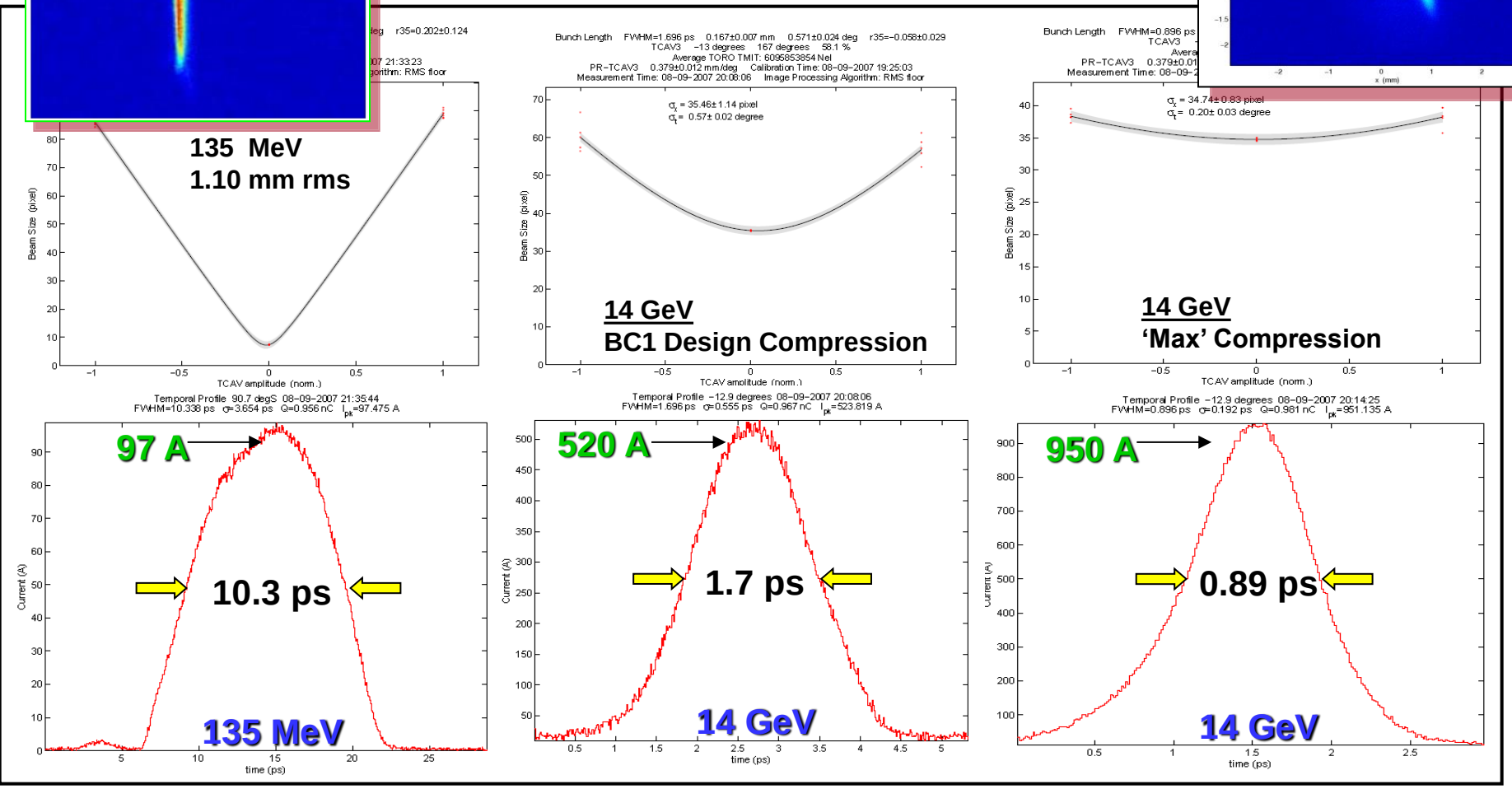

Transverse deflector (TCAV)

Bunch length
Destructive (*)
Single Shot

Resolution : $\sigma_z > \sqrt{\frac{\gamma \varepsilon_n}{\beta_{TCAV}}} \left(\frac{\lambda_{rf}}{eV_o}\right) \left(\frac{m_o c^2}{2\pi}\right)$

Resolution	Tech	P[MW] V[MV]	L[m]	E[MeV]	ε [mm-mrad]/β [m]	Loc.
250 fs	S-Band (1)	0.5/0.7	0.4	135	0.3/5	LCLS inj.
11 fs (3)	S-Band	?/15	2.44	5000	0.5/60	LCLS main
33 fs	X-Band (2)	1/?	0.13	100	1/11	XTA
1 fs	X-Band	40/?	2.0	4300		LCLS dump
3 fs	X-Band	40 /?	2.0	14000		LCLS dump

(1) S-Band is 2.856 GHz
(2) X-Band is 11.424 GHz
(3) Measured on wire scanner

(*) pulse stealing on LCLS (1Hz for a 120Hz operation)

Transverse deflector (TCAV)

Bunch length
Destructive
Single Shot

Longitudinal Phase space

Destructive (but "stealing mode") Single Shot

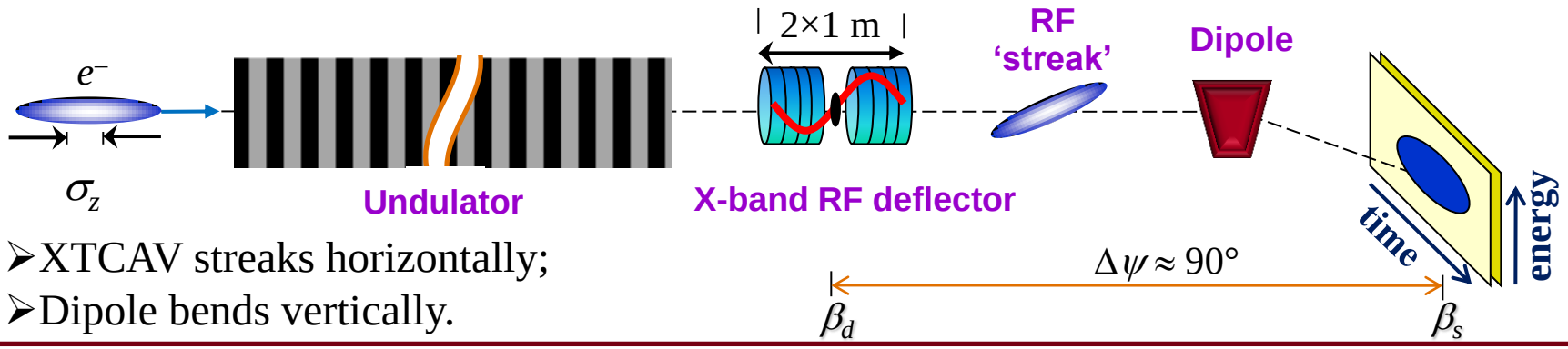

- XTCAV streaks horizontally;
- Dipole bends vertically.

Longitiudinal Phase space

Bunch length
Destructive
Single Shot

Initial Measurement of e-beam and X-ray temporal profiles at LCLS using X-Band transverse deflector

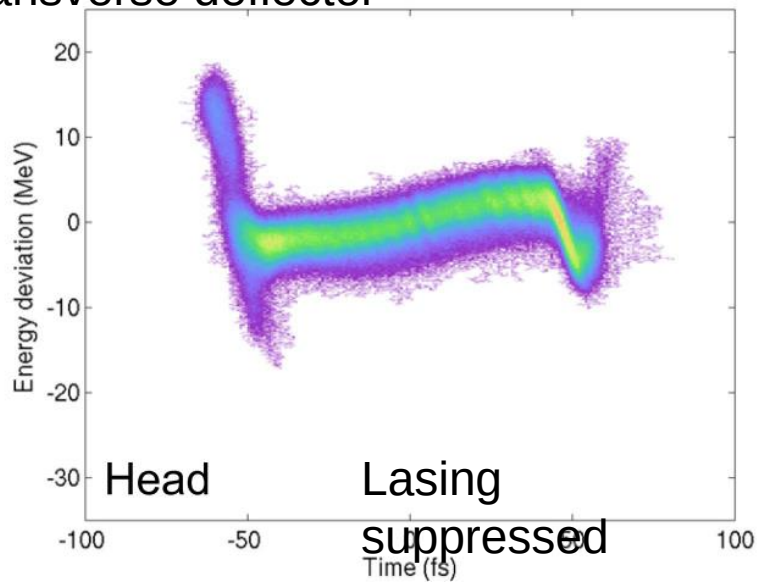

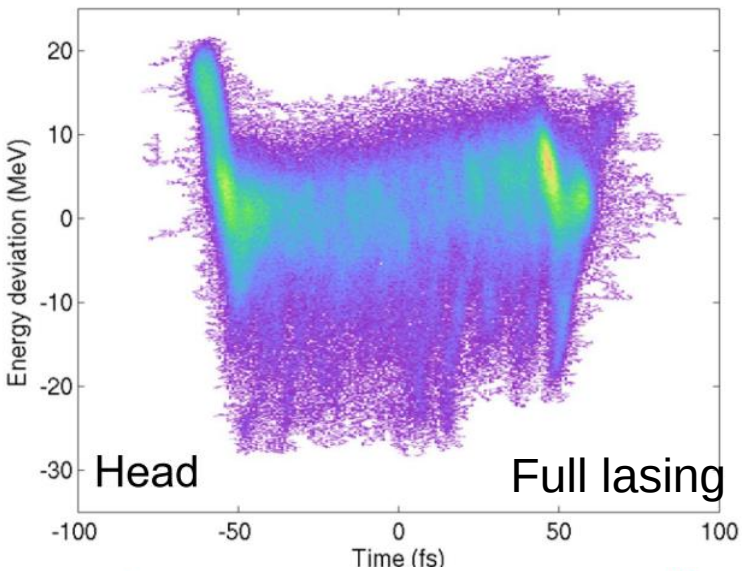

Data taken on June 4th, 2013.
Beam energy 3.5GeV, 150pC.
Temporal resolution is about 1.7fs rms in this test.

Preliminary results.

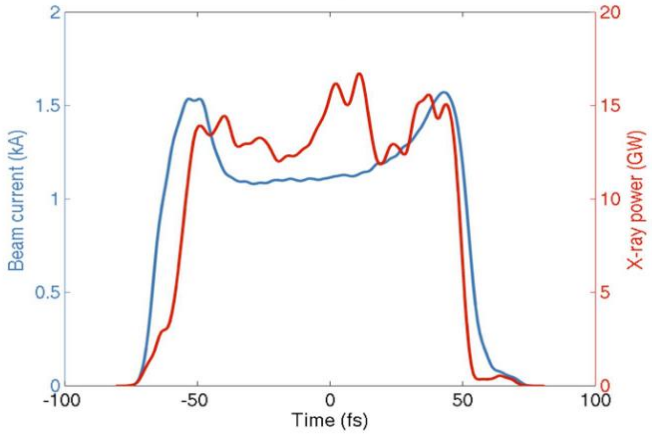

Longitudinal Phase space end LCLS injector

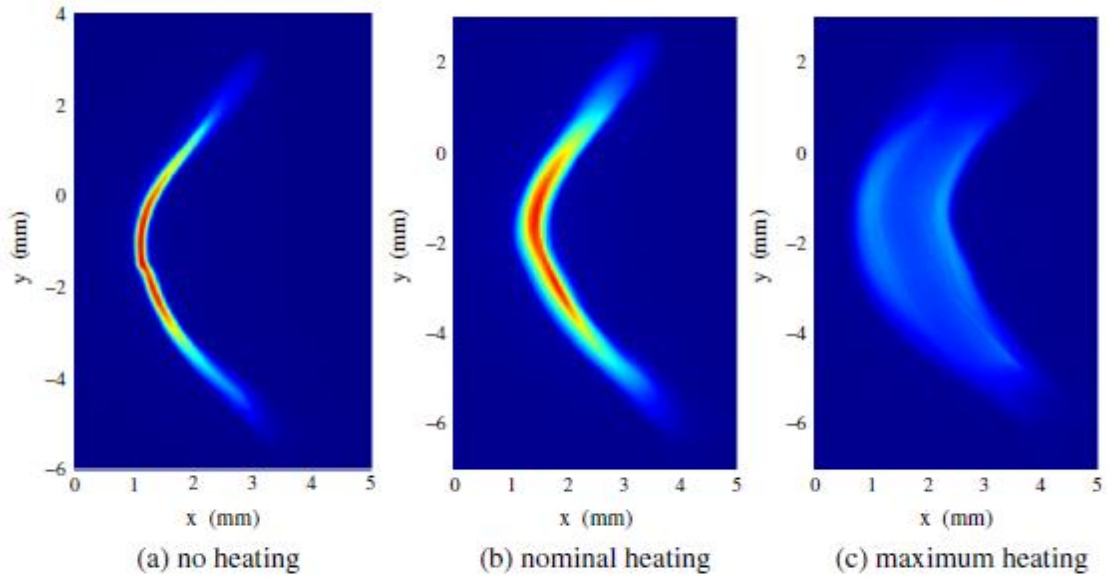

FIG. 5. (Color) Measured longitudinal phase space on "YAGS2" screen at 135 MeV with (a) laser heater off, (b) IR-laser energy at 10 μJ, and (c) at 220 μJ.

Z.Huang, Phys. Rev. ST Accel. Beams 13, 020703 (2010)

Acknowledgments

C.Pellegrini, D.Xiang, T.Raubenheimer

H.Loos, T.Maxwell, M.Ross, D.McCormick, G.White, A.Marinelli, Y.Ding, P.Emma, P.Krejcik, J.Wu

J.O.Luiten, J.Yan, F.LePimpec, R.Gantry, F.Zimmermann, M.Minty , S.Anderson, C.Hauri, A.Anghel, B.Steffen, B.Schmidt, A.Cianchi, A.Cavalieri, R.Li, W.Engelen, R.Fiorito, K.Rezaie, A.Nause, T.Shintake, P. Tenenbaum, D.Dowell, G.Berden, C.Casalbuoni, H.Tomizawa,

…

and all the students

Topics of interest

- Tomography
- Optical Replica
- Synchronization

Electro-Optic Sampling

Bunch length
Non-destructive
Single Shot

T.Maxwell

http://accelconf.web.cern.ch/accelconf/IPAC2011/papers/tupc169.pdf

http://www.niu.edu/physics/_pdf/academic/grad/theses/Maxwell_2012.pdf

B.Steffen

http://fla.desy.de/projects/eo/index_eng.html

http://www-library.desy.de/cgi-bin/showprep.pl?thesis07-020

Casalbuoni

http://prst-ab.aps.org/pdf/PRSTAB/v11/i7/e072802

Synchronization (AOS-based)

Non-destructive Single Shot

Cavalieri

http://prl.aps.org/abstract/PRL/v94/i11/e114801